spectrum. The assigned systematic uncertainties in this case would then be

(1) uncertainty in stopping rate, $\pm 15\%$;
(2) uncertainty in neutron rate from source, $\pm 10\%$;
(3) uncertainty due to energy spectrum, $\pm 10\%$.

The final multiplicity values become 1.0 ± 0.4 for Na and 0.6 ± 0.2 for Mg.

At the present time, it is possible to compare only the Pb multiplicity with other independent determinations. Since the primary interest of this experiment is not in Pb and not in the absolute values of the multiplicity, we merely quote such a comparison in Table VII.

We reiterate here the principal conclusions of the experiment, aside from the numerical values already quoted. They are that the neutron multiplicities due to μ mesons' stopping in Mg and Na are clearly nonzero and the Na value is very probably less than that for Pb but greater than that for Mg. The indicated relative multiplicity values for Na and Mg are consistent with the particular hypothesis that influenced the choice of absorber, namely, the view that the meson-nucleus interaction process favors a relatively large angular momentum change. Further experimental work is desirable to improve our understanding of this interaction.

The author wishes to express his sincere thanks to Professor R. D. Sard for his continued help and encouragement, to Dr. M. Annis for his valued assistance and suggestions, and to Mr. J. D. Miller for his work with the electronics.

PHYSICAL REVIEW VOLUME 105, NUMBER 5 MARCH 1, 1957

Pion Production in Electron-Proton Collisions*

R. H. DALITZ,† *University of Birmingham, Birmingham, England*

AND

D. R. YENNIE, *Stanford University, Stanford, California*

(Received November 5, 1956)

The close relationship between photopion and electropion production from protons allows an unambiguous first estimate (the standard value) for the ratio of these cross sections, based on assumptions very close to those of the Weizsäcker-Williams method. Deviations of the ratio from this estimate arise from pion production by the longitudinal components of the field of the scattered electron and from the variation of the off-diagonal transverse excitations from their diagonal photoproduction values. The dependence of these deviations on the physical processes contributing to the electromagnetic excitation of pions is discussed in terms of matrix elements specified in the pion-nucleon center-of-mass system, both for various phenomenological contributions and for specific meson theories. The experimental values reported are interpreted as an indication of the smallness of longitudinal production, in qualitative accord with the fixed source theory. These features may also be investigated by study of the energy spectrum of inelastically scattered electrons and of the azimuthal variation of pion production relative to the scattering plane, which are also discussed here.

1. INTRODUCTION

MEASUREMENTS on direct pion production by electrons incident on hydrogen have recently been made by Panofsky, Woodward, and Yodh.[1] Since this pion production is induced by the action of the virtual electromagnetic field of the scattered electron, it is closely related to the photoproduction of pions from hydrogen. However, in contrast to photoproduction, the energy k_0 transferred by this virtual field is not necessarily equal to the momentum transfer k. Furthermore, while the electromagnetic field in the photoproduction process is transverse, the virtual electromagnetic field in the electron-production process contains both transverse and longitudinal components. For these reasons, it is expected that the experimental results will contain new information on the electromagnetic properties of the pion-nucleon system.

The close relation between the interactions produced by a moving charged particle and those due to incident electromagnetic waves was first pointed out in 1924 by Fermi,[2] who related stopping power for α particles to the electromagnetic properties of the material. Weiz-

* The research reported here was supported in part by the U. S. Air Force through the Air Force Office of Scientific Research, Air Research and Development Command, and was also sponsored by the joint program of the Office of Naval Research and the U. S. Atomic Energy Commission.

† This research was begun at Stanford University under the joint program of the Office of Naval Research and the U. S. Atomic Energy Commission and was continued under the same program at Cornell University. This author enjoyed support, also, as a member of the Institute for Advanced Study and as a Visiting Associate Physicist at Brookhaven National Laboratory during the progress of this work.

[1] Panofsky, Woodward, and Yodh, Phys. Rev. **102**, 1392 (1956).

[2] E. Fermi, Z. Physik **29**, 315 (1924).

säcker and Williams[3] later considered particularly the case of relativistic electrons. By making a Fourier analysis of the field produced at a given point by a passing electron of energy ϵ and momentum $p \gg m$, they showed that this field contained predominantly transverse components and concluded that an incident electron would produce the same effects as a beam of photons with spectrum $N_e(p,k_f)$ given by

$$N_e(p,k_f)(dk_f/k_f) = \frac{\alpha}{\pi}\frac{dk_f}{k_f}\{z^2[K_1^2(z)-K_0^2(z)]-2zK_0(z)K_1(z)\}. \quad (1.1)$$

Here k_f is the photon energy, $z=(\mathrm{mb}_{\min}k_f/\epsilon)$, $b_{\min}$ is the least impact parameter for which the electron is effective in the given process, and K_0, K_1 are the usual Bessel functions. This discussion assumes that the electron motion is not appreciably affected by the process induced, in particular that the scattering angle of the electron is small. The contribution from field components parallel to the incident direction is omitted in this approximation. A convenient approximation to Eq. (1.1), valid for $z \ll 1$, is

$$N_e(p,k_f)=(2\alpha/\pi)[\ln(\epsilon/k_f)-\ln(\mathrm{mb}_{\min})-0.39]. \quad (1.2)$$

Nordheim *et al.*[4] have made a more detailed classical analysis of the virtual field of the uniformly-moving electron by Fourier analyzing the field considered as a function of space and time. This analysis shows clearly that the least impact parameter $b_{\min}$ is to be taken as $1/k_{\max}$, where $k_{\max}$ is the greatest transverse momentum transfer strongly effective in the process.[5] This momentum transfer may be as large as $k_{\max}\approx p$; but if R is the radius of the region over which the electromagnetic interaction with the system is strong, then $k_{\max}R \lesssim 1$. Generally the appropriate $b_{\min}$ is given in order of magnitude by the larger of R and $1/p$. For very high electron energies, experimental results on the relative effectiveness of electron and photon in a given process will give direct information on this radius R of strong interaction, according to Eq. (1.2).

In the Stanford experiments, the electron energy (600 Mev) is not large compared with the energy transfer to the pion-nucleon system. Also the pion-production process is quite complex, a number of different transitions being effective. Thus, while Eq. (1.2) is adequate for an order-of-magnitude estimate, a more precise treatment is needed for the interpretation of the experiments. Such a treatment may be based on the Møller potential for the scattered electron. For energy and momentum transfer $k_0, \mathbf{k}$, this potential has components

$$A_\mu(k_0,\mathbf{k})=e\frac{\bar{u}(\mathbf{p}-\mathbf{k})\gamma_\mu u(\mathbf{p})}{k_0^2-k^2}, \quad (1.3)$$

where $k_0=\epsilon(\mathbf{p})-\epsilon(\mathbf{p}-\mathbf{k})$. The interaction of this potential with the pion-nucleon system may be denoted by

$$H'(\mathbf{k})=J_\mu(k_0,\mathbf{k})A_\mu(k_0,\mathbf{k}), \quad (1.4)$$

where $J_\mu(k_0,\mathbf{k})$ is the matrix element of the current operator for the system between initial nucleon and final pion-nucleon states.

First consider the case of an infinitely heavy nucleon. For a given pion energy the energy of the scattered electron $[\epsilon'=\epsilon(\mathbf{p}-\mathbf{k})]$ is definite. The ratio of the total cross section for the electron process to that for the corresponding photon process may then be calculated by using Eqs. (1.3) and (1.4) to give[6]

$$N_e(p,k_f)=N_e{}^t(p,k_f)+N_e{}^l(p,k_f), \quad (1.5)$$

where

$$N_e{}^t(p,k_f)=\frac{\alpha}{\pi}\int_{(p-p')^2}^{(p+p')^2}\frac{k_f^2 d(k^2)}{(k_0^2-k^2)^2}\times\left\{\frac{[(p+p')^2-k^2][k^2-(p-p')^2]}{4p^2k^2}+\frac{k^2-k_0^2}{2p^2}\right\}\times\frac{\langle J_t^2(k^2)\rangle}{\langle J_t^2(k_f^2)\rangle}. \quad (1.5a)$$

$$N_e{}^l(p,k_f)=\frac{\alpha}{\pi}\int_{(p-p')^2}^{(p+p')^2}\frac{k_f^2 d(k^2)}{4k_0^2p^2}\times\left\{\frac{(p+p')^2}{k^2}-1\right\}\frac{\langle J_l^2(k^2)\rangle}{\langle J_l^2(k_f^2)\rangle}. \quad (1.5b)$$

In this equation, $\mathbf{k}=\mathbf{p}-\mathbf{p}'$ and $k^2=p^2+p'^2-2pp'\cos\theta$, θ being the electron scattering angle. Neglecting the electron's mass, the momentum of the real photon is equal to that of the virtual photon for forward electron scattering: $k_f=p-p_f'$. In Eq. (1.5), $\langle J_t^2\rangle$ denotes the square of the part of $\mathbf{J}(k_0,\mathbf{k})$ transverse to $\mathbf{k}$, averaged over initial and final nucleon spins, over meson directions and over the two photon polarizations; $\langle J_l^2\rangle$ denotes the square of the longitudinal part of $\mathbf{J}(k_0,\mathbf{k})$, similarly averaged. The last term in each of the curly brackets of Eq. (1.5) is due to the electron magnetic moment. The invariant quantity

$$k_0^2-k^2=2(m^2-\epsilon\epsilon'+pp'\cos\theta) \quad (1.6)$$

has the small value $\approx -m^2(p-p')^2/pp'$ for forward scattering ($\theta=0$). The main (logarithmic) contribution to $N_e(p,k_f)$ therefore comes from the region $k^2\approx k_0^2$, owing to the denominator $(k_0^2-k^2)^2$ of the first integral. This corresponds to small-angle electron scattering and transverse production only and can be predicted without further knowledge of the pion process. Knowledge of

[3] K. F. Weizsäcker, Z. Physik **88**, 612 (1934); E. J. Williams, Phys. Rev. **45**, 729 (1934); Kgl. Danske Videnskab. Selskab, Mat.-fys. Medd. **13**, 4 (1935).

[4] Nordheim, Nordheim, Oppenheimer, and Serber, Phys. Rev. **51**, 1037 (1937).

[5] We use units such that $\hbar=c=1$.

[6] See the remarks following Eq. (2.14).

off-the-energy-shell matrix elements ($k^2>k_0^2$) for interaction with the transverse and longitudinal fields is necessary for the complete evaluation of $N_e(p,k_f)$. The additional contribution clearly corresponds to relatively large electron scattering angles. Because of this additional contribution, $N_e(p,k_f)$ will depend on the model considered as well as on the energies involved. It is these differences which interest us here.

The simplest estimate of $N_e(p,k_f)$ is obtained by (i) giving $\langle J_t^2(k^2)\rangle$ the value it has on the energy shell, i.e., the value $\langle J_t^2(k_f^2)\rangle$ effective in photoproduction; (ii) omitting the longitudinal matrix elements $\mathbf{J}_l$. This estimate will be referred to as the "standard value" of $N_e(p,k_f)$ and is explicitly

$$N_e^{st}(p,k_f)=\frac{\alpha}{\pi}\left\{\frac{\epsilon^2+\epsilon'^2}{p^2}\ln\frac{\epsilon\epsilon'+pp'+m^2}{m(\epsilon-\epsilon')}-\frac{(\epsilon+\epsilon')^2}{2p^2}\ln\frac{p+p'}{p-p'}-\frac{p'}{p}\right\}. \quad (1.7)$$

The contributions to Eq. (1.7) come very predominantly from small scattering angles; e.g., for $p=600$ Mev/c, $k_f=200$ Mev, 95% of the integral comes from scattering angles less than 6°. The physical situation for this case therefore corresponds closely to the approximations of Weizsäcker and Williams[7]; and this expression (1.7), which is based on the use of the Møller potential, may be regarded as a more quantitative generalization of Eq. (1.2).

The function $N_e(p,k_f)$ of Eq. (1.5) has frequently been calculated for special cases in the past, although not presented in this form. Electrodisintegration of the deuteron was considered by Bethe and Peierls,[8] assuming only an electric dipole transition; this is equivalent to the assumptions that the longitudinal and transverse matrix elements $\langle J_t^2\rangle$ and $\langle J_l^2\rangle$ are equal and are independent of k^2. Such relations between longitudinal and transverse matrix elements are typical only of physical situations such that $kR\ll 1$. For situations where the momentum transfer is such that $kR>1$, the transverse and longitudinal matrix elements may have quite different magnitudes and k dependences. This is, for example, the case for pion production where k necessarily exceeds μ, and may be illustrated by the explicit calculations of Sec. 3. Higher multipoles have been discussed by Wick,[9] without specification of the particular nuclear process involved; these expressions are again valid only for electron energies such that $kR\ll 1$. For the magnetic dipole or transverse electric quadrupole transitions, $N_e(p,k_f)$ has the value

$$\frac{\alpha}{\pi}\frac{\epsilon^2+\epsilon'^2}{p^2}\ln\frac{\epsilon\epsilon'+pp'+m^2}{m(\epsilon-\epsilon')} \quad (1.8)$$

corresponding to $\langle J_t^2\rangle\propto k^2$. A longitudinal $E2$ transition may also be effective and will add

$$\frac{2\alpha}{\pi}\frac{p'^2}{(\epsilon-\epsilon')^2}\eta^2 \quad (1.9)$$

to the transverse contribution (1.8), where η^2 is the ratio $\langle J_l^2(k_f^2)\rangle/\langle J_t^2(k_f^2)\rangle$ of the effectiveness of longitudinal $E2$ to transverse $E2$ transitions at $k=k_f$. The value of η^2 is 4/3 for any system such that $k_{\max}R\ll 1$. This expression is in fact valid only as long as $k_{\max}R\ll 1$ and may be very large if $(\epsilon-\epsilon')\ll p$. This is particularly the case for the excitation of low-lying quadrupole transitions in nuclei by electrons of moderate energy (<30 Mev) where η^2 will be equal to 4/3. From Eq. (1.5) it is clear that large contributions then come from large values of k^2, i.e., from large-angle electron scattering. Formulas for the case of an octupole transition have been given by Thie *et al.*[10]

In the process $e+p\rightarrow n+\pi^++e$, the electron loses a large proportion of its energy and therefore delivers considerable momentum to the pion-nucleon system. In the experiments of Panofsky *et al.*, observations are made of pions with definite directions and energy; in a photoproduction process these observations on the pion suffice to determine the kinematics completely, but this is not so for the electron process where there are three particles in the final state. However, the final electron energy is a definite function of its direction. For forward scattering its energy loss is very closely equal to k_f, the photon energy necessary to produce a pion of this momentum and direction from a proton which is initially at rest. Since small-angle scattering contributes so strongly in Eq. (1.5), a reasonable second approximation $N_e^{st}(p,k_f)$ is simply obtained by neglecting the variation of p' with scattering angle in Eq. (1.5), replacing p' everywhere by the value $p'(\theta=0)=p-k_f$ which it has for forward scattering. The values then obtained are significantly less than those obtained in the approximation $p'=p-\omega_q$ corresponding to the assumption of an infinitely heavy nucleon (see Table I).

However, as the electron scattering angle becomes large, the neutron recoil necessarily increases so that the final electron energy falls appreciably. For large angles the momentum transfers k are therefore smaller

[7] For an "equivalent-photon" energy $k_f\ll p$, Eq. (1.7) reduces to $N_e^{st}(p,k_f)=(2\alpha/\pi)[\ln(p/m)-0.5]$. This agrees with Eq. (1.2) for the choice $b_{\min}=1/k_f$. For $b_{\min}=1/p$, however, Eq. (1.2) gives N_e rather larger than the standard value. This increase is due to the fact that the Weizsäcker-Williams calculation comprises the contributions of the matrix elements transverse to the incident direction. Since the momentum transfers actually make some angle with this direction in general, some contributions corresponding to matrix elements longitudinal to the momentum transfer are consequently included in the semiclassical calculation, but are omitted in the calculation of the standard value $N_e^{st}(p,k_f)$.

[8] H. A. Bethe and R. E. Peierls, Proc. Roy. Soc. (London) **A148**, 146 (1935).

[9] G. C. Wick, Ricerca sci. **11**, 49 (1940). See also B. Peters and C. Richman, Phys. Rev. **59**, 804 (1941), and J. S. Blair, Phys. Rev. **75**, 907 (1949).

[10] Thie, Mullen, and Guth, Phys. Rev. **87**, 962 (1952).

and the energy transfers larger than with the assumption of constant energy loss k_f; further, the phase space for the final electron is now diminished for large-angle scattering and the value of N_e is further decreased. For the standard value, small-angle scattering contributes so predominantly that the decrease due to the variation of neutron recoil with scattering angle θ is quite small, being between 2% and 3% for all physical situations of interest at present.

It will now be clear that the new information on the pion-nucleon interaction contained in experimental values of N_e depends only on its deviation from the standard value N_e^{st}. This deviation may depend on (i) the variation of the transverse matrix element with increasing momentum transfer $k>k_0$, for given energy transfer k_0; (ii) the effectiveness of longitudinal production. Contributions to N_e from these causes necessarily correspond to values k^2 considerably greater than k_0^2, and therefore to large-angle scattering. These deviations are consequently affected greatly by the variation of neutron recoil with electron scattering angle and will be very much less than the values suggested by the above formulas, Eqs. (1.8) and (1.7), for example, in which a constant $p'=p-k_f$ is assumed. This reduction follows both from the reduction in the momentum transfers effective for large-angle scattering and from the decrease in the phase space available to the final electron. This is particularly marked for the longitudinal $E2$ production, Eq. (1.9), whose large value depended so strongly on large-angle scattering. The remarks are illustrated quantitatively in Table I by consideration of some typical cases of interest here.

The values of N_e do not have a simple relation to the new pion-nucleon matrix elements of interest but depend on integrals over these off-the-energy-shell matrix elements. Complementary information on these matrix elements would be given by experiments in which the spectrum of inelastically-scattered electrons at a given angle is observed. This latter situation will be discussed briefly in Sec. 4; experiments of this type are in progress at Stanford. In the interpretation of the electron-pion results, it is necessary to take account of the on-the-energy-shell transverse matrix elements deduced from the more complete data on pion photoproduction. The guidance of successful meson theories is also needed, although these experiments depend on situations for which the validity of these theories may be in doubt. In these experiments at 600 Mev, momentum transfers effective in electroproduction may be as large as $\approx Mc$ (M is the nucleon mass). The matrix elements may be expected to fall rapidly for k such that $kR>1$, where R is the radius of the region of strong electromagnetic interaction for the pion-nucleon system. At present we have very little knowledge of the appropriate radius R for the various transitions, and it is just in this region that our theories may be least valid. However, preliminary estimates of off-diagonal electromagnetic matrix elements will be made is Sec. 3 on the basis of simple treatments of pseudoscalar meson theory.

TABLE I. Values of $N_e(p,k_f)$ calculated for $P=600$ Mev and $k_f=228.2$ Mev (appropriate to 60-Mev pions observed at 75° to the beam) with various kinematical assumptions. The matrix elements used are the simple forms appropriate for $kR\ll 1$. The various assumptions relating the longitudinal and transverse matrix elements are labeled (lab), (c.m.), and (c.m.)* and are defined in Sec. 2.

$N_e(p,k_f)$		Nucleon assumed infinitely heavy	Variation of nucleon recoil neglected	With correct kinematics	Correct kinematics and a matrix element (Yukawa shape) with rms radius $R=1.0$ $\times 10^{-13}$ cm	$R=2.0$ $\times 10^{-13}$ cm
Standard value		0.0216	0.0207	0.0200	0.0192	0.0181
Electric dipole	(lab)	0.0253	0.0237	0.0214	0.0201	0.0187
	(c.m.)	···	···	0.0254	0.0218	0.0193
	(c.m.)*	···	···	0.0226	0.0209	0.0190
Magnetic dipole	(lab)	0.0284	0.0265	0.0238	0.0212	0.0191
	(c.m.)	···	···	0.0238	0.0212	0.0191
Electric quadrupole	(lab)	0.0536	0.0430	0.0283	0.0238	0.0202
	(c.m.)	···	···	0.0506	0.0323	0.0226
	(c.m.)*	···	···	0.0337	0.0264	0.0212

Previous calculations of electroproduction of pions on the basis of meson theory are rather incomplete. It has generally been assumed that the nucleon is infinitely heavy, the corresponding kinematics being used; this leads to a quite considerable error in the interesting part of N_e. The total cross section for all meson production has been considered by Feshbach and Lax[11] using the Weizsäcker-Williams approximation, and by Strick and ter Haar,[12] who give the threshold behavior $\sigma_{\text{tot}}(\epsilon)\propto(\epsilon-\epsilon_0)^{\frac{3}{2}}$. For the fixed-source pseudoscalar theory, Sneddon and Touschek[13] have given expressions (calculated in Born approximation) for the meson spectrum, integrated over angles, neglecting all nucleon recoil effects. Further, these authors have explicitly omitted the longitudinal terms in the matrix elements. Kaplon[14] has given more complete expressions for the differential cross section, but again with neglect of longitudinal production and recoil effects. The recoil will of course have its greatest effect through the kinematics of the process and the resulting phase-space factors.

2. GENERAL FORMULATION

In this section we shall derive some general expressions for the electron production of pions, and apply them to a simplified treatment of the process. In Eq. (1.4), the matrix element for pion production by an electromagnetic field has been expressed in terms of the

[11] H. Feshbach and M. Lax, Phys. Rev. **76**, 134 (1949).
[12] E. Strick and D. ter Haar, Phys. Rev. **78**, 68 (1950).
[13] I. N. Sneddon and B. Touschek, Proc. Roy. Soc. (London) **A199**, 352 (1949).
[14] M. F. Kaplon, Ph.D. thesis, University of Rochester, 1951 (unpublished). See also R. E. Marshak, *Meson Physics* (McGraw-Hill Book Company, Inc., New York, 1952), p. 40.

current j_μ associated with the transition from nucleon to final pion-nucleon state. Using charge conservation

$$k_0 j_0 - \mathbf{k}\cdot\mathbf{j} = 0, \tag{2.1}$$

the fourth component of j_μ can be expressed in terms of the space components; here k_0, $\mathbf{k}$ are the energy and momentum transfer in the transition. Similarly the Møller potential, Eq. (1.3), satisfies the Lorentz condition

$$k_0 A_0 - \mathbf{k}\cdot\mathbf{A} = 0. \tag{2.2}$$

Using these two relations, the matrix element for the transition may be written

$$H' = \mathbf{j}\cdot\mathbf{A} - k_0^{-2}\mathbf{k}\cdot\mathbf{j}\mathbf{k}\cdot\mathbf{A}. \tag{2.3}$$

It is now convenient to separate the current into a longitudinal component

$$\mathbf{j}_l = \mathbf{k}\mathbf{k}\cdot\mathbf{j}/k^2, \tag{2.4}$$

and transverse component $\mathbf{j}_t$, so that

$$\mathbf{j} = \mathbf{j}_t + \mathbf{j}_l. \tag{2.5}$$

Then H' can be written in the compact form

$$H' = \mathbf{m}\cdot\mathbf{A}, \tag{2.6}$$

where $\mathbf{m}_t = \mathbf{j}_t$ and $\mathbf{m}_l = \mathbf{j}_l(1-k^2/k_0^2)$.

In terms of $\mathbf{m}$, the differential cross section for the production of a pion of momentum $\mathbf{q}$ is

$$\delta(\epsilon'+\omega_q+E-\epsilon-M) \times \frac{\alpha m^2}{(k^2-k_0^2)^2}\frac{1}{64\pi^4}\sum|\langle\gamma_i m_i\rangle|^2\frac{M}{E}\frac{d^3p'}{p\epsilon'}\frac{d^3q}{\omega_q}, \tag{2.7}$$

where the sum is to be taken over initial and final spin states for the electron and the nucleon. Here E is the energy of the recoil neutron

$$E = [M^2+(\mathbf{p}-\mathbf{p}'-\mathbf{q})^2]^{\frac{1}{2}}. \tag{2.8}$$

The appearance of the factor (M/E) in (2.7) is a consequence of assuming that the nucleon wave functions are normalized relativistically in calculating the matrix elements $\mathbf{j}$. Since we do not have an adequate relativistic theory for $\mathbf{m}$, there is some question whether it is appropriate to include this factor; it is convenient to include it since the phase space expression for the final particles then has simple transformation properties.

Since only the meson is observed in the present experiments, Eq. (2.7) is to be integrated over all possible final electron states. For each electron scattering angle, the electron's energy is fixed by the conservation laws [see Eq. (2.14)] below, so that the integration is over electron directions only. The result is to be compared with the corresponding expression for photoproduction by a bremsstrahlung spectrum $\phi(K)dK/K$, which is

$$\delta(\omega_q+E-K-M)\frac{\phi(K)dK}{K}\frac{1}{64\pi^2 K}\sum|\langle m_t\rangle|^2\frac{M}{E}\frac{d^3q}{\omega_q}, \tag{2.9}$$

the sum being over the two photon polarizations and the nucleon spin states. For given $\mathbf{q}$, the appropriate value of K is $k_f = \epsilon - \epsilon_f'$, where ϵ_f' is the energy of the final electron for forward scattering ($\theta = 0$).

Let T_{ij} denote the sum over electron spins in Eq. (2.7):

$$T_{ij} = m^2\sum[\bar{u}(\mathbf{p})\gamma_i u(\mathbf{p}-\mathbf{k})][\bar{u}(\mathbf{p}-\mathbf{k})\gamma_j u(\mathbf{p})] = 2p_i p_j - p_i k_j - p_j k_i + \tfrac{1}{2}(k^2-k_0^2)\delta_{ij}. \tag{2.10}$$

Then the remaining sum may be written

$$\Phi_e = (\sum T_{ij}m_i^* m_j)(k^2-k_0^2)^{-1} = \mathrm{Tr}\{2|\mathbf{p}\cdot\mathbf{m}_t|^2 + \tfrac{1}{2}(k^2-k_0^2)|\mathbf{m}_t|^2 + 2\,\mathrm{Re}(\mathbf{p}\cdot\mathbf{m}_t\mathbf{k}\cdot\mathbf{m})(p^2-p'^2)/k^2 + \tfrac{1}{2}[-1+(p+p')^2/k^2](k_0^2/k^2)|\mathbf{k}\cdot\mathbf{m}|^2\} \times (k^2-k_0^2)^{-1}. \tag{2.11}$$

The trace here is with respect to the nucleon spin. The corresponding expression for photoproduction is

$$\Phi_{\mathrm{ph}} = \mathrm{Tr}(\mathbf{m}_t^*\cdot\mathbf{m}_t)_f. \tag{2.12}$$

The subscript f denotes that the current is evaluated for $K = k_f$.

The ratio of the meson intensity produced by electron bombardment to that produced by bremsstrahlung will be denoted by $N_e/\phi(K)$ where, from Eqs. (2.7) and (2.9),

$$N_e(p,k_f) = \frac{\alpha}{\pi}\frac{4k_f^2}{pp_f'}\int\frac{\Phi_e}{\Phi_{\mathrm{ph}}}\frac{p'^2}{(k^2-k_0^2)}\frac{d\Omega}{4\pi}, \tag{2.13}$$

where p_f' is the momentum of the recoil electron for forward scattering. Specifying the electron scattering angle by θ, the angle between $\mathbf{p}$ and $\mathbf{p}'$, and ϕ, the angle between the planes $(\mathbf{p},\mathbf{q})$ and $(\mathbf{p},\mathbf{p}')$, the final electron momentum is given by

$$p' = \frac{M(p-\omega_q)+p(q\cos\alpha-\omega_q)+\frac{1}{2}\mu^2}{M+p-\omega_q-p\cos\theta+q(\cos\alpha\cos\theta+\sin\alpha\sin\theta\cos\phi)}. \tag{2.14}$$

This expression is correct to order (m^2/p'^2); the angle of pion emission relative to the incident direction is α. Typical curves of p' have been given in reference 1. The expression (1.5) for total cross sections may be obtained from Eq. (2.13) by replacing p' by the constant value p_f' everywhere and integrating numerator and denominator over all meson directions; the cross term between transverse and longitudinal production averages to zero in the total cross section.

In the calculation of N_e for some models it is sometimes more convenient to proceed without separation of the transverse and longitudinal parts of the interaction current. For these cases it may be convenient to use the covariant form

$$\Phi_e = \tfrac{1}{2}\,\mathrm{Tr}[\bar{j}_\mu j_\mu + |\bar{p}_\mu j_\mu|^2(k^2-k_0^2)^{-1}], \tag{2.15}$$

where $\bar{j}_\mu j_\mu = |j_1|^2+|j_2|^2+|j_3|^2-|j_0|^2$, and $\bar{p}_\mu = p_\mu + p_\mu'$. This form may be obtained directly from Eqs.

(1.3) and (1.4) by using covariant projection operators in the usual way for evaluation of the sum over electron spin states. An equivalent form is

$$\Phi_e=\tfrac{1}{2}\,\mathrm{Tr}[\tilde{\jmath}_\mu j_\mu+(4/k_0^2)(\mathbf{b}\cdot\mathbf{j}^*)(\mathbf{b}\cdot\mathbf{j})(k^2-k_0^2)^{-1}], \quad (2.16)$$

where $\mathbf{b}=\epsilon'\mathbf{p}-\epsilon\mathbf{p}'$. To a close approximation, this vector $\mathbf{b}$ is perpendicular to the bisector of the angle between $\mathbf{p}$ and $\mathbf{p}'$ and lies in the plane of $\mathbf{p}$ and $\mathbf{p}'$ (see Fig. 1, reference 1). In each of these expressions (2.15) and (2.16) the virtual photons may be regarded as consisting of an unpolarized part giving rise to the first term and a polarized part responsible for the second term.

The expression (2.15) for Φ_e is explicitly a relativistic invariant. Hence, despite their noncovariant appearance, the equivalent expressions (2.11) and (2.16) must each have the same value in every Lorentz frame provided the value $\mathbf{j}$ appropriate to that frame is used. Now, even in a relativistic theory, the discussion of the final pion-nucleon state is most conveniently carried through in a particular Lorentz system, the pion-nucleon center-of-mass (c.m.) system, and by consideration of scattering states which have definite angular momentum and parity in this system. The matrix elements calculated for a nonrelativistic fixed-source theory, which neglects the motion of the nucleon, are best used in this c.m. system where neglect of the nucleon motion is most justified. The corresponding matrix element for calculation of Φ_e in some other Lorentz frame must then be obtained by a Lorentz transformation; if the fixed-source matrix element is used directly in another Lorentz frame, a different approximation is being made and a different value will be obtained for Φ_e. It is clearly desirable therefore to evaluate Φ_e in a Lorentz frame which varies with the electron scattering angle, namely, the c.m. system of the virtual photon and target nucleon (which is of course identical with the final pion-nucleon c.m. system). In this Lorentz frame we shall denote the various momenta by capital letters corresponding to the lower-case letters used in the laboratory system; thus $\mathbf{Q}$ and $\mathbf{K}$ will denote the pion momentum and the momentum transfer of the virtual photon as seen in the pion-nucleon c.m. system.

However it is most convenient to carry out calculations using the variables defined directly in the laboratory frame. Since the c.m. system has velocity $\mathbf{k}/(M+k_0)$ relative to the laboratory, the energy and momentum transfers K_0, $\mathbf{K}$ seen in the c.m. system may be expressed in terms of the laboratory quantities $k_0,\mathbf{k}$:

$$K_0=\frac{k_0(M+k_0)-k^2}{\{[(M+k_0)^2-k^2]\}^{\frac{1}{2}}},$$
$$\mathbf{K}=\mathbf{k}\frac{M}{\{[(M+k_0)^2-k^2]\}^{\frac{1}{2}}}. \quad (2.17)$$

These expressions necessarily satisfy the relation $K_0^2-K^2=k_0^2-k^2$. Similarly, it is clear that the transverse components of current in the two systems are equal,

$$j_t=J_t, \quad (2.18a)$$

while the relation between the longitudinal components is

$$j_0/k_0=J_0/K_0, \quad (2.18b)$$

taking account of Eq. (2.1). With these relations (2.18), direct computation of (2.11) yields the same value in either of these Lorentz frames, confirming the remarks of the previous paragraph.

The first case of interest is transverse electric-dipole excitation. The assumption of a point dipole corresponds to a constant matrix element J_t, with $J_l=0$; with Eqs. (2.18), the current in the laboratory system also has constant j_t, and $j_l=0$. The value N_e then obtained is just the standard value; the result for a typical case is given in Table I. Results are also given on the same line of the table for a transverse dipole of finite interaction volume (or corresponding form factor) specified in the c.m. system.

For longitudinal excitation, a point electric-dipole (E.D.) interaction giving a constant matrix element $J_l=J_t$ in the c.m. system corresponds to a matrix element $j_l=j_tk_0/K_0$ in the laboratory system, following Eq. (2.18). The c.m. assumption "equal transverse and longitudinal matrix elements."

$$\text{E.D. (c.m.)}: J_t(K)=J_t(K_f),\ J_l(K)=J_t(K_f), \quad (2.19a)$$

therefore leads to a quite different result from the corresponding assumption,

$$\text{E.D. (lab.)}: j_t(k)=j_t(k_f),\ j_l(k)=j_t(k_f), \quad (2.19b)$$

in the laboratory frame, as shown also in Table I. In fact for the case considered, the longitudinal contribution with (2.19a) is about four times that obtained for (2.19b). This large difference can be traced to the fact that $k_0\gg K_0$ at the larger angles. From Eq. (2.1), it is clear that the assumption $J_l=$constant, necessarily requires J_0 to be very large when K_0 is small. For sufficiently high electron energy and a sufficiently large scattering angle it is possible for K_0 to pass through zero and become negative; clearly both J_0 and $\mathbf{J}$ should remain finite for all K, K_0 so that we can conclude that $J_l\to 0$ as $K_0\to 0$. Thus the more appropriate assumption for J_l is that it has the form K_0 times a slowly varying function of K and K_0. For electric-dipole excitation, the simplest such assumption is then

$$\text{E.D. (c.m.)}^*: J_t(K)=J_t(K_f),\quad J_l(K)=J_t(K_f)K_0/K_f, \quad (2.19c)$$

for which the N_e obtained is intermediate between those for the original assumptions (2.19a) and (2.19b).

Higher multipole moments correspond to the use of form factors vanishing for $K=0$ in the present approximation where the multipole moments are assumed to

have no dependence on the pion momentum. For magnetic dipole (M.D.) excitation, a point dipole corresponds to form factors

$$\text{M.D. (c.m.)}: \; J_t(K)=J_t(K_f)K/K_f, \; J_l(K)=0. \quad (2.20)$$

As shown by Table I, essentially the same result for N_e is obtained for a k/k_f dependence, corresponding to a point magnetic dipole in the laboratory system. For electric-quadrupole (E.Q.) excitation, the transverse part is identical with the magnetic-dipole case, but there is also the longitudinal excitation; with "equal transverse and longitudinal matrix elements,"

$$\text{E.Q. (c.m.)}: \; J_t(K)=J_t(K_f)K/K_f, \quad J_l(K)=J_t(K_f)K/K_f, \quad (2.21a)$$

$$\text{E.Q. (c.m.)*}: \; J_t(K)=J_t(K_f)K/K_f, \quad J_l(K)=J_t(K_f)KK_0/K_f^2. \quad (2.21b)$$

Following the discussion of the last paragraph, the latter expression gives the simplest reasonable assumption. For this case there is an especially large difference between this expression, the expression (2.21a) and the assumption

$$\text{E.Q. (lab.)}: \; j_t(k)=j_l(k)=j_t(k_f)k/k_f, \quad (2.21c)$$

in the laboratory frame. Owing to the heavy weighting of the contributions from the large-angle scattering, the longitudinal contributions are completely different for each of these cases. For each situation listed in Table I, it is the value labeled with asterisk which corresponds to the most reasonable treatment of the longitudinal contributions.

Except for electric dipole excitation near threshold, these models are all too crude to explain pion production by electrons. However, they serve to illustrate the pitfalls associated with the improper treatment of nucleon recoil. Except for the relativistic weak coupling theory[15] and the relativistic Tamm-Dancoff theory,[16] there are at present no treatments of the electromagnetic production of pions which do properly take nucleon recoil into account. Since the nucleon recoil will not be unimportant in the c.m. system for large-angle scattering, this introduces an additional uncertainty in the discussion of the matrix elements in this region.

3. CALCULATION OF N_e

A. Phenomenological Treatment

We first describe the process phenomenologically, following the method of Brueckner and Watson,[17] and Gell-Mann and Watson.[18] The separation of the interaction into terms corresponding to states of definite angular momentum and parity is rigorous and well defined in the c.m. system; however the dependence of the strengths of the various terms on the energy and momentum of the virtual photon are, of course, not known in advance.

In the cases of present interest, the pion-nucleon relative energy is sufficiently low for consideration of S and P waves alone to suffice. For S-wave pion production, both transverse and longitudinal electric dipole transitions may be effective. The corresponding matrix elements may be written

$$iD_t(\boldsymbol{\sigma}-\mathbf{K}\boldsymbol{\sigma}\cdot\mathbf{K}/K^2)+iD_l\mathbf{K}\boldsymbol{\sigma}\cdot\mathbf{K}/K^2, \quad (3.1)$$

where the coefficients D_t, D_l are independent functions of K^2 and Q^2 (or K^2 and K_0). In photoproduction, only the transverse term D_t is effective, and also there is a definite relation between K^2 and Q^2. For production of mesons in the $P_{\frac{1}{2}}$ state, a monopole transition is possible in addition to the magnetic dipole transition effective in photoproduction, giving terms

$$(M_1/KQ)(-\mathbf{Q}\times\mathbf{K}-i\mathbf{Q}\boldsymbol{\sigma}\cdot\mathbf{K}+i\boldsymbol{\sigma}\mathbf{Q}\cdot\mathbf{K}) +i(O_l/KQ)\mathbf{K}\boldsymbol{\sigma}\cdot\mathbf{Q}. \quad (3.2)$$

Finally there are the transitions to the $P_{\frac{3}{2}}$ state, the magnetic dipole M_3 and transverse electric quadrupole E_t terms effective in photoproduction and also a longitudinal electric quadrupole term E_l

$$(M_3/KQ)(-2\mathbf{Q}\times\mathbf{K}+i\mathbf{Q}\boldsymbol{\sigma}\cdot\mathbf{K}-i\boldsymbol{\sigma}\mathbf{Q}\cdot\mathbf{K}) +i(E_t/KQ)(\mathbf{Q}\boldsymbol{\sigma}\cdot\mathbf{K}+\boldsymbol{\sigma}\mathbf{K}\cdot\mathbf{Q}-2\mathbf{K}\boldsymbol{\sigma}\cdot\mathbf{K}\mathbf{K}\cdot\mathbf{Q}/K^2) +i(E_l/KQ)(2\boldsymbol{\sigma}\cdot\mathbf{K}\mathbf{K}\cdot\mathbf{Q}/K^2-2\boldsymbol{\sigma}\cdot\mathbf{Q}/3)\mathbf{K}. \quad (3.3)$$

We are concerned here specifically with the production of positive pions, so that these matrix elements do not refer to definite isotopic spin states. In terms of matrix elements to final states $T_{\frac{1}{2}}$ and $T_{\frac{3}{2}}$, each of the terms above, X_α, has the form[18]

$$X_\alpha=[X_{\alpha 3}\exp(i\delta_{\alpha 3})+\sqrt{2}X_{\alpha 1}\exp(i\delta_{\alpha 1})]/\sqrt{3}, \quad (3.4)$$

where $\delta_{\alpha\tau}$ denotes the pion-nucleon scattering phase shift for isotopic spin $\tau/2$ in the final orbital state to which X_α leads and the amplitudes $X_{\alpha\tau}$ are real. For neutral pion production, the corresponding matrix elements $X_\alpha^{(0)}$ are given by

$$X_\alpha^{(0)}=[\sqrt{2}X_{\alpha 3}\exp(i\delta_{\alpha 3})-X_{\alpha 1}\exp(i\delta_{\alpha 1})]/\sqrt{3}. \quad (3.5)$$

The phenomenological analysis of charged and neutral pion photoproduction given by Watson and collaborators has led to considerable knowledge of the transverse matrix elements on the energy shell $K^2=K_0^2$. The dominant matrix elements are the S-wave excitation D_t and the enhanced matrix elements M_{33} and E_{t3} leading to the resonant (33) state; the most complete information on the magnitudes of E_{t3}, M_{33}, and D_t has

[15] See, for example, Marshak,[14] p. 4.
[16] Dyson, Ross, Salpeter, Schweber, Sandaresen, Visscher, and Bethe, Phys. Rev. **95**, 1644 (1954); Marc Ross, Phys. Rev. **94**, 455 (1954); **103**, 760 (1956).
[17] K. A. Brueckner and K. M. Watson, Phys. Rev. **86**, 923 (1952).
[18] M. Gell-Mann and K. M. Watson, *Annual Review of Nuclear Science* (Annual Reviews, Inc., Stanford, 1952), Vol. 4, p. 219.

been given recently by Watson *et al.*[19] The other transverse matrix elements are relatively small and are important mainly through their interference with the terms above. These results will be used as a guide in discussion of electroproduction of pions; the interpretation will depend on the form of these dominant matrix elements for $K^2>K_0^2$, and on the effectiveness of the longitudinal terms.

Even though it has not been expressed in a covariant form, this description of the electromagnetic production of pions in terms of multipole moments is quite rigorous. It is assumed that the four-component Dirac spinor has been reduced to two-component form by expressing the two "small" components in terms of the two "large" ones. All the terms arising from this reduction, as well as the relativistic normalization factors, are included in the definition of the X_α's; the remaining two-component spinors are normalized to unity. Of course we do not actually have available the covariant form of J_μ for carrying out this reduction, but we know from angular momentum and parity considerations in the c.m. frame that the result must be in the form of Eqs. (3.1) through (3.3) for the lowest few states. In a more general Lorentz frame, such a simple expansion as this would no longer hold because the total momentum of the system gives an additional vector which would appear in the various angular factors of the expansion. It happens that an expansion of this form does hold in the laboratory frame since the total momentum is parallel to $\mathbf{k}$; however, in passing between the laboratory frame and the c.m. frame the multipole moments become mixed together. [According to Eqs. (2.19) and (2.20), the separation into longitudinal and transverse parts would remain invariant in passing between these two frames.] From these considerations, we believe the c.m. frame is the preferred one for a phenomenological calculation. Some of the kinematical relations and formulas required for such a calculation are given in the Appendix.

A difference from the situation considered in the Introduction is that the direction $\mathbf{q}$ of the pion is observed. Even for a particular multipole transition and a definite momentum transfer $\mathbf{k}$, the angular distribution of the pion relative to $\mathbf{k}$ differs from that for photoproduction owing to the p dependence of T_{ij} [see Eq. (2.11)]. This distribution has next to be averaged over all momentum transfers effective, with appropriate weighting, so that the pion angular distribution in electroproduction will differ somewhat from the photoproduction distribution. In addition, the longitudinal transitions effective in electroproduction will have different angular distributions.

[19] Watson, Keck, Tollestrup, and Walker, Phys. Rev. **101**, 1159 (1956). {Evidence on π^0 photoproduction presented by D. R. Corson at the Rochester Conference [*Proceedings of the Sixth Annual Rochester Conference on High-Energy Physics* (Interscience Publishers, Inc., New York, 1956)] indicates that E_{l3} is much smaller than given by the analysis of Watson *et al.*}

Because of the large number of unknown functions occurring in Eqs. (3.1) through (3.4), it seems impractical at the present time to use the phenomenological treatment for making anything better than very crude estimates of N_e. This will be carried out by direct numerical calculation of (2.13) using the complete expression for Φ_e (given in terms of c.m. quantities in the appendix) corresponding to the sum of the matrix elements (3.1), (3.2), and (3.3). For purposes of illustration we present here the result obtained for the transitions M_3, E_t, and E_l leading to the resonant state, when recoil is neglected.

$$\begin{aligned}\bar{\Phi}_e{}^P = p^2\{&[(2+3\sin^2\alpha)|M_3|^2+2\,\mathrm{Re}(M_3{}^*E_t)(1-3\cos^2\alpha)\\&+|E_t|^2(1+\cos^2\alpha)]X+(4/9)|E_l|^2(1+3\cos^2\alpha)Y\\&+[(3\cos^2\alpha-1)/2][(3|M_3|^2-|E_t|^2)V\\&+8\,\mathrm{Re}(M_3{}^*E_t)W-4\,\mathrm{Re}(M_3{}^*E_l+\tfrac{1}{3}E_t{}^*E_l)Z\\&-(4/3)|E_l|^2Y\sin^2\sigma]\},\end{aligned}\tag{3.6}$$

where

$$\begin{aligned}X&=(2p^2)^{-1}+\sin^2\sigma/(k^2-k_0^2),\\Y&=[(p+p')^2-k^2](k^2-k_0^2)/2k_0^2k^2p^2,\\Z&=(\epsilon+\epsilon')\cos\sigma\sin^2\sigma/kk_0p,\\V&=\sin^2\sigma/2p^2,\\W&=2X\sin^2\sigma-V/2,\end{aligned}$$

and σ is the angle between the momentum transfer $\mathbf{k}$ and the beam direction. This angle is related to the momentum transfer by

$$\sin^2\sigma=[(p+p')^2-k^2][k^2-(p-p')^2]/4k^2p^2.\tag{3.7}$$

In Eq. (3.6) the integration over ϕ has already been carried out; this integration corresponds roughly to the averaging over polarizations in the photoproduction process. The square-bracket coefficient of X in (3.6) is in fact the photoproduction distribution function Φ_{ph}. It will be noticed that the pion angular distributions for the pure excitations differ from those for photoproduction. The functions X and Y appear also as factors in the integrals (1.5); this is natural since, on integration over α, the cross terms of Eq. (3.6) vanish and the expressions (1.5) are regained. Each of the functions Z, V, and W vanishes in the forward direction $\sigma=0$, $k=k_f\cong k_0$, so that the additional terms in the pion angular distribution arise from relatively large-angle electron scattering.

For S-wave excitation, the corresponding expression is

$$\bar{\Phi}_e{}^S=2|D_t|^2X+|D_l|^2Y.\tag{3.8}$$

This is essentially the same as Eq. (2.18) if we place $\lambda_t=|D_t/D_{tf}|$ and $\lambda_l=|D_l/D_{tf}|$. The result is exactly as discussed in Sec. 2 and tabulated in Table I for some simple assumptions about D_t and D_l. The transverse $P_{\frac{1}{2}}$ excitation will be neglected. Although it leads to a state of weak scattering, the interesting longitudinal $P_{\frac{1}{2}}$ excitation O_l may be comparable with D_l (see Fig. 1) for pion energies considered here and it is therefore

included since it will contribute a positive addition to N_e; it should be added here that O_l has no interference with M_{33}.

The function $\Phi_{\rm ph}$ equals the sum of the coefficients of X in (3.6) and (3.8), the matrix elements being taken on the energy shell for forward scattering, $k^2=k_f^2$. Deviation of $N_e(p,k_f)$ from the standard value will then arise from the variation of M_{33}, E_{t3}, and D_t with momentum transfer k^2, from the interference terms of Eq. (3.6), and from the longitudinal production terms of Eqs. (3.6) and (3.8). On the energy shell, D_t and M_{33} are dominant matrix elements: it is possible that E_{t3} is also "enhanced," and that E_{t3}/M_{33} is roughly 0.5 over a large energy range across the resonance.[19] In the numerical calculation the following momentum dependences were assumed for the various multipole moments: $D_t\propto$ const; $D_l\propto K_0$; $M_1\propto KQ$; $O_l\propto KQK_0$; $M_3\propto KQ$; $E_t\propto KQ$; and $E_l\propto KQK_0$. This is necessarily their behavior for small K, Q, and K_0 (see Sec. 2) and would continue for large values if the interaction volume were sufficiently small. Since there is a finite interaction volume, there will be "form factors" and there will also be the phase factors of Eqs. (3.4) and (3.5) which depend on the energy of the meson in the c.m. frame and vary slightly from angle to angle. At the present stage only two experimental numbers are available, so that it is clearly not possible to provide a unique interpretation of the result without theoretical guidance, even following the "enhancement model." Simple meson theoretical considerations will be discussed in the following subsections, and the interpretation will be discussed in Sec. 5.

B. Fixed-Source Pion Theory of Chew

In this subsection, the current $\mathbf{J}$ associated with the pion production will be considered according to the linear fixed-source theory of pseudoscalar pions. On the basis of this theory, Chew and collaborators[20] have given a rather successful account of the data available on pion-nucleon scattering and pion photoproduction. Here it is the ratio of production of pions of definite energy and direction by electrons and by photons which is of interest. This ratio will depend on rather broad features of $\mathbf{J}$: the relative magnitude of its longitudinal part and the momentum dependence of its transverse part.

For reasons which have been discussed by Kroll and Ruderman,[21] the Born approximation for $\mathbf{J}$ is adequate near the pion-production threshold. This is given by

$$\mathbf{J}=\frac{\sqrt{2}eg}{2M}\left[\boldsymbol{\sigma}-(2\mathbf{Q}-\mathbf{K})\frac{\boldsymbol{\sigma}\cdot(\mathbf{Q}-\mathbf{K})}{\mu^2+(\mathbf{Q}-\mathbf{K})^2}\right] \tag{3.9}$$

for π^+ production. As the pion energy increases, modifications to this become important especially because of the resonant interaction in the (33) state. However, since S-state scattering is weak, it seems reasonable to use the S-wave part of Eq. (3.9) up to quite high energies; for photoproduction, Watson *et al.*[19] have shown that this provides an adequate account of the data. Equation (3.9) contains two terms of distinct physical origin. The first refers to the production of pions which have interacted with virtual nucleon pairs and are therefore produced at a radius of order $1/M$. The second term describes photoejection from the meson cloud of the proton; these pions are produced at relatively larger radii[22] up to $1/\mu$. The second term therefore has considerable k dependence.

The S-wave current may be obtained from Eq. (3.9) by averaging over the direction of Q, leading to the form (3.1) where

$$D_t=1-(Q/2K)[I_0(\Lambda)-I_2(\Lambda)], \tag{3.10a}$$

$$D_l=1-(K/2Q)[I_0(\Lambda)-3(Q/K)I_1(\Lambda)+2(Q/K)^2I_2(\Lambda)], \tag{3.10b}$$

and $\Lambda=(\omega_Q^2+K^2)/2QK$. The functions I_n are given by the recurrence relation

$$I_n(\Lambda)=\Lambda I_{n-1}(\Lambda)-[1-(-1)^n]/2n, \tag{3.11}$$

with $I_0(\Lambda)=\frac{1}{2}\ln[(\Lambda+1)/(\Lambda-1)]$. At threshold ($Q=0$), D_t is unity and $D_l=\mu^2/(\mu^2+K^2)$; on the energy shell ($K=\mu$), D_l/D_t equals one-half and with increasing K^2, D_l falls rapidly while D_t remains constant. Thus at threshold the transverse contribution to $N_e(p,k_f)$ is just the standard value; the total $N_e(p,k_f)$ is slightly greater than the standard value because of the longitudinal contribution. Above threshold both D_t and D_l depend on the momentum transfer K; typical curves of these and the other multipole moments are shown in Fig. 1. Generally, the second term of D_t is quite small as only pions at relatively large radii can be ejected effectively by the transverse field; however, D_t increases with K^2, and this causes the transverse contribution to N_e to exceed the standard value slightly. On the other hand, the two terms of D_l tend to cancel for large K, the second term being large (of order one) because pions at rather small radii in the cloud have a strong interaction with the longitudinal field. Generally, D_l is appreciably smaller than D_t on the energy shell ($K=\omega_Q$) and falls rapidly with increasing momentum transfer K^2.

The fixed-source theory is, of course, not relativistically invariant. Following the discussion of Secs. 2 and 3A it is most reasonable to use the matrix elements of such a theory in the c.m. frame, rather than the laboratory frame. At our present energies, the energy transfer K_0 in this c.m. frame becomes rather small over a certain region of electron-scattering angles; the longitudinal current should vanish with K_0, whereas the fixed-source matrix element is independent of K_0. To include

[20] The results are summarized by G. F. Chew, Phys. Rev. **95**, 1669 (1954).

[21] N. M. Kroll and M. A. Ruderman, Phys. Rev. **93**, 233 (1954).

[22] In pseudoscalar theory the pion cloud is somewhat singular, with dependence $e^{-\mu r}/r^2$ so that radii $<\hbar/\mu c$ do play an important role.

the dominant K_0 dependence, whose importance has been emphasized in Sec. 2, the longitudinal part of the current (3.9) is multiplied by the factor (K_0/K_f), the transverse current being unmodified: this factor is unity for forward scattering. For the case of the Born-approximation matrix element (3.9), this procedure will be justified by examination of the relativistic Born approximation in the next subsection: the remaining relativistic corrections to both transverse and longitudinal parts of $\mathbf{J}$ should be quite small under present experimental conditions.

The Chew-Low matrix element is obtained from a treatment of photoproduction based on field-theoretic methods developed recently by Low.[23] This method has the great advantage that it deals only with physically observable quantities, but it has been developed for photoproduction only as far as the "one-meson" approximation. Chew and Low[24] have pointed out the dominant modification to Eq. (3.9) which arises from this approximation; this is the addition of a magnetic-moment term

$$\frac{\sqrt{2}eg}{2M}D_0(2i\mathbf{Q}\times\mathbf{K}+\boldsymbol{\sigma}\cdot\mathbf{K}\mathbf{Q}-\boldsymbol{\sigma}\mathbf{Q}\cdot\mathbf{K})\times\frac{e^{i\delta_{33}}\sin\delta_{33}}{Q^3/\mu}F(K^2); \quad (3.12)$$

where

$$D_0=\tfrac{1}{3}(\mu/4M)(4\pi/f^2)(g_p-g_n)=0.7\pm0.1.$$

The factor $F(K^2)$ is the form factor for the nucleon magnetic moment, as given by Chew and Low. Since rather little is known of this form factor, we shall take $F=1$ for the present situation.[25] Chew and Low then show that the sum of Eqs. (3.9) and (3.12) is able to account directly for certain outstanding and well-known features of pion photoproduction. However, this matrix element does not include a modification to the $E2$ matrix element for final-state scattering. The $E2$ term included in Eq. (3.9) has phase zero instead of δ_{33} and will not interfere with (3.12) near resonance.

Calculation of $N_e(p,k_f)$ may now be made by substituting this expression for $\mathbf{J}$ into Eq. (2.11) and integrating Eq. (2.13). Complete expressions for Φ_e are given in the appendix and the results will be discussed in Sec. 5.

The fixed-source theory may also be considered in the Tamm-Dancoff approximation.[16] In this form the theory of pion processes has less elegance than in the Chew-Low approximation; the problem of renormalization involves considerable complication in practice, and calculations have not been carried through to include as much as is included in the one-meson approximation

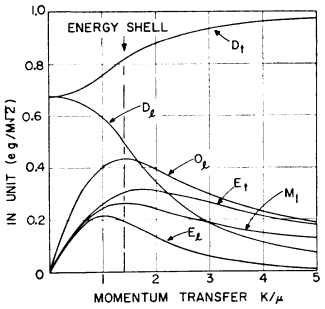

FIG. 1. Matrix elements for production of positive pions of (c.m.) energy 55.4 Mev as a function of momentum transfer K, calculated for various multipoles in Born approximation from the expression (3.9).

of Chew and Low. However, the features of interest in our problem may be illustrated in a familiar physical way by use of the Tamm-Dancoff theory in its simplest form. The desired matrix element is that of the current operator of the pion-nucleon system between initial nucleon and final state of interacting pion and nucleon. In the simplest Tamm-Dancoff theory, no more than one pion is allowed in the nucleon's pion cloud and the final state is represented by the Tamm-Dancoff wave function of the pion-nucleon system. After taking into account the isotopic spin dependence of the pion-nucleon interaction, this results in the following expression for the amplitude for production of positive pions,

$$\frac{1}{3}\int\left\{\psi_{Q,\frac{1}{2}}^*(\mathbf{S})\frac{1}{(\omega_S)^{\frac{1}{2}}}[\mathbf{J}^+(\mathbf{S},\mathbf{K})+\sqrt{2}\,\mathbf{J}^0(\mathbf{S},\mathbf{K})]+\psi_{Q,\frac{1}{2}}^*(\mathbf{S})\frac{1}{(\omega_S)^{\frac{1}{2}}}[2\mathbf{J}^+(\mathbf{S},\mathbf{K})-2\mathbf{J}^0(\mathbf{S},\mathbf{K})]\right\}\times(\omega_Q)^{\frac{1}{2}}d_3S. \quad (3.13)$$

In this expression, $\mathbf{J}^+(\mathbf{S},\mathbf{K})$ and $\mathbf{J}^0(\mathbf{S},\mathbf{K})$ denote the current amplitude for production of positive and neutral pion of momentum $\mathbf{S}$, respectively, and $\psi_{Q,T}(\mathbf{S})$ is the final-state wave function for the c.m. motion of a pion-nucleon system of isotopic spin T, $m_T=+\frac{1}{2}$, and of pion momentum $\mathbf{Q}$. The foregoing expression (3.9) gives the dominant term of $\mathbf{J}^+$. The neutral amplitude $\mathbf{J}^0$ arises mainly from higher order corrections which describe the interaction of the electromagnetic field with the nucleon magnetic moment. This term is proportional to $(\mu_p-\mu_n)$ and is naturally appreciable only for magnetic transitions. However $\mathbf{J}^0$ contributes strongly to the π^+ production only when the final-state scattering is strong: for states of weak interaction, $\psi_{\frac{3}{2}}\equiv\psi_{\frac{1}{2}}$ and the terms $\mathbf{J}^0$ cancel in Eq. (3.13). The magnetic moment interaction is therefore important only for the $M1$ excitation of the resonant (33) state: it is indeed just this effect which is estimated by the additional term (3.12) of Chew and Low. The contribution of the magnetic moments to $\mathbf{J}^+$ will be neglected here since it is proportional to the small quantity $(\mu_p+\mu_n)$.

The amplitude (3.12) may now be expressed as a sum of the amplitudes (3.1), (3.2), and (3.3) for various

[23] F. E. Low, Phys. Rev. **97**, 1392 (1955).
[24] G. F. Chew and F. E. Low, Phys. Rev. **101**, 1597 (1956).
[25] Electron scattering experiments at Stanford indicate that the rms radius of the magnetic-moment distribution in the proton is about 0.7×10^{-13} cm. This work is reported in R. W. McAllister and R. Hofstadter, Phys. Rev. **102**, 851 (1956), and E. E. Chambers and R. Hofstadter, Phys. Rev. **103**, 1454 (1956).

multipole excitations. The contribution of the (33) state to the final-state wave function $\psi_{Q,\frac{3}{2}}(\mathbf{S})$ is, for example,

$$e^{i\delta_{33}}\cos\delta_{33}(\boldsymbol{\sigma}\cdot\mathbf{Q}\times\mathbf{S}-2i\mathbf{Q}\cdot\mathbf{S})\phi_Q(S), \quad (3.14)$$

where $\phi_Q(S)$ has the form

$$\phi_Q(S)=\delta(Q-S)+P\frac{F_Q(S)\tan\delta_{33}(Q)}{\omega_Q-\omega_S}. \quad (3.15)$$

In Eq. (3.15), P denotes principal value integration over the singularity and $F_Q(S)$ is the function obtained from the Tamm-Dancoff calculation of pion-nucleon scattering.[26] The contribution of (3.14) to (3.13) may now be separated into the three multipole terms of (3.3), each of the coefficients having the form

$$e^{i\delta_{33}}[B(K,Q)\cos\delta_{33}+T(K,Q)\sin\delta_{33}], \quad (3.16)$$

where $B(K,Q)$ is the Born approximation matrix element for this particular multipole and $T(K,Q)$ is the corresponding final-state integral over $F_Q(S)$. The importance of this form (3.16) for the photoproduction matrix elements has been discussed particularly by Ross.[16]

The $E2$ excitations of the resonant state may now be considered. These estimates are of particular interest since the $E2$ excitations have not yet been calculated in the Chew-Low approximation. The Born approximation amplitudes may be obtained from (3.9), and are given explicitly by

$$B(E_t)=-\frac{eg\sqrt{2}}{2M}\times\left\{\tfrac{3}{4}[I_0(\Lambda)-I_2(\Lambda)]-\frac{3Q}{2K}[I_1(\Lambda)-I_3(\Lambda)]\right\}, \quad (3.17)$$

$$B(E_l)=-\tfrac{1}{2}B(E_t)-\frac{eg\sqrt{2}}{2M}\frac{3K}{4Q}\times\left[I_1(\Lambda)-3\left(\frac{Q}{K}\right)^2 I_2(\Lambda)+2\left(\frac{Q}{K}\right)^2 I_3(\Lambda)\right]. \quad (3.18)$$

For these $E2$ excitations, $T(K,Q)$ has been calculated numerically using Tamm-Dancoff wave functions obtained by Salzman and Snyder.[26] A typical curve of $B(K,Q)$ and $T(K,Q)$ as a function of the momentum transfer K for pion energy near the resonance is shown in Fig. 2 for both E_t and E_l. In Born approximation, the pions tend to be produced in outer regions of the nucleon cloud, so that $B(K,Q)$ tends to fall off as the momentum transfer increases beyond the energy shell, and inner regions of the cloud are explored. This decrease of $B(K,Q)$ is especially marked for the longitudinal transition E_l. Now the pion-nucleon interaction in pseudoscalar theory becomes increasingly stronger for closer and closer approach, so that contributions from the inner regions of the cloud are more strongly enhanced above Born approximation than are the outer contributions. Consequently the matrix element $T(K,Q)$ will continue to rise for larger momentum transfers K than $B(K,Q)$, owing to this singular attraction between pion and nucleon in the final state.

Finally, the $P_{\frac{1}{2}}$ excitations are to be considered. Since the pion-nucleon scattering is weak in the $P_{\frac{1}{2}}$ states, the final-state effects will be neglected here. For the $M1$ excitation, the matrix element is given by

$$B(M_1)=-\frac{eg\sqrt{2}}{2M}\tfrac{1}{2}[I_0(\Lambda)-I_2(\Lambda)]. \quad (3.19)$$

There is also the monopole excitation

$$B(O_l)=\frac{eg\sqrt{2}}{2M}\left[\tfrac{1}{2}I_0(\Lambda)+I_2(\Lambda)-\left(\frac{Q}{K}+\frac{K}{2Q}\right)I_1(\Lambda)\right]. \quad (3.20)$$

These matrix elements are plotted as a function of K in Fig. 1 for a pion-nucleon relative energy of 55 Mev. It is of interest to note that, at this energy, O_l and D_l are comparable on the energy shell, and that, in general, O_l decreases much less rapidly than D_l with increasing K. At this energy then, since E_l is small and falls rapidly with increase of K, it follows that the greater part of the longitudinal production of pions may be expected to arise from the monopole excitation. At higher energies, near resonance, the quadrupole excitation may be expected to contribute to the longitudinal production and to interfere with the dominant resonance excitation.

C. Relativistic Born Approximation

Owing to the uncertainties arising from the nonrelativistic character of fixed-source pion theory, as discussed in Secs. 2 and 3b, it is of some interest to examine briefly the matrix element of the relativistic weak-coupling theory, the relativistic counterpart to

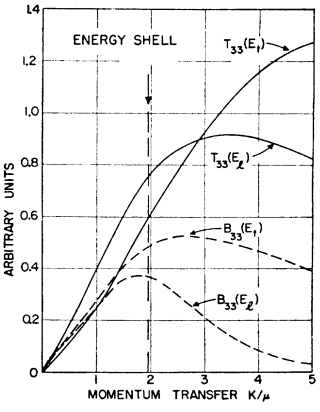

FIG. 2. Matrix elements for electric quadrupole excitation of π^+ production near resonance (pion c.m. energy 126 Mev) as function of momentum transfer K.

[26] J. L. Gammel, Phys. Rev. **95**, 209 (1954); F. Salzman and J. Snyder, Phys. Rev. **95**, 286 (1955); M. Kalos and R. H. Dalitz, Phys. Rev. **100**, 1515 (1955).

expression (3.8). This takes the form

$$J_\mu = eg\sqrt{2}\bar{\psi}(\mathbf{s})\gamma_5 \times\left[\frac{1}{\mathbf{r}-\mathbf{k}-iM}\gamma_\mu - \frac{2q_\mu - k_\mu}{(q_\lambda - k_\lambda)^2+\mu^2}\right]\psi(\mathbf{r}), \quad (3.21)$$

where $\psi(\mathbf{r})$ denotes the four-spinor for momentum $\mathbf{r}$ and $\bar{\psi}=\psi^\dagger\gamma_0$ is its adjoint.

In the c.m frame, the initial and final nucleons have momenta $-\mathbf{K}$ and $-\mathbf{Q}$, respectively. For comparison with the phenomenological and fixed-source theories, it is convenient to express the current $\mathbf{J}$ in this frame in terms of Pauli spin functions by the replacement

$$\psi(\mathbf{P}) = V_P(1+i\gamma_5\boldsymbol{\sigma}\cdot\mathbf{R}_P)u, \quad (3.22)$$

where $\mathbf{R}_P=\mathbf{P}/(E_P+M)$ and $V_P=[(E_P+M)/2M]^{\frac{1}{2}}$. With this replacement, the current matrix element becomes

$$\mathbf{J} = ieg\sqrt{2}\left[\frac{\boldsymbol{\sigma}}{E+M} - \frac{\boldsymbol{\sigma}\cdot\mathbf{R}_Q\boldsymbol{\sigma}\cdot\mathbf{R}_K}{E-M} + \frac{(2\mathbf{Q}-\mathbf{K})\boldsymbol{\sigma}\cdot(\mathbf{R}_Q-\mathbf{R}_K)}{(E_Q-E_K)^2-\omega_Q{}^2-K}\right]V_K V_Q, \quad (3.23)$$

the energy relation being $K_0+E_K=E_Q+\omega_Q=E$. It may readily be verified that expression (3.23) reduces to the previous fixed-source expression (3.9) when the nonrelativistic limit $Q, K\ll M$ is taken for the nucleon.

Consider in particular the longitudinal part of $\mathbf{J}$, which may be written

$$\mathbf{J}\cdot\mathbf{K} = ieg\sqrt{2}\frac{K_0}{K_{\rm ph}} \times\left(\boldsymbol{\sigma}\cdot\mathbf{R}_Q\frac{E+M}{2E}\left\{1-\frac{(E-M)(\omega_Q+E_K-E_Q)}{\omega_{Q-K}{}^2-(E_Q-E_K)^2}\right\} + \boldsymbol{\sigma}\cdot\mathbf{R}_K\left\{-\frac{E-M}{2E}+\frac{(\omega_Q+E_K-E_Q)(E^2-M^2)}{2E[\omega_{Q-K}{}^2-(E_Q-E_K)^2]}\right\}\right), \quad (3.24)$$

where $K_{\rm ph}=(E^2-M^2)/2E$ is the photon energy necessary to produce this final pion-nucleon state in the center-of-mass system. For the energies of interest at present, the fixed-source limit $K, Q\ll M$ provides a quite good approximation for the terms within the curly brackets of Eq. (3.24); however the factor $(K_0/K_{\rm ph})$ outside can change very greatly (and even change sign) from its fixed-source value of unity for quite moderate Q, K such that the fixed-source limit is elsewhere quite adequate. It should be added here that a corresponding examination of the transverse current shows that no significant error is made (at present energies) in going to the fixed-source limit.

For direct calculation of N_e with the covariant matrix element (3.21), any convenient Lorentz frame may be used for evaluation of Φ_e, using expressions (2.15) or (2.16). It is in fact most direct to carry calculation through in the laboratory frame: expressions are given in the appendix for the quantities occurring in Φ_e, and the results of numerical calculations for the cases of interest will be discussed in Sec. 5.

4. INELASTIC ELECTRON-PROTON SCATTERING

Complementary information bearing directly on the off-diagonal behavior of the current matrix element $\mathbf{J}$ may be obtained from the measurement of the spectrum of electrons inelastically scattered into a particular direction after pion production from protons. Since the energy transfer k_0 from the electron to the struck system is related to the momentum transfer k by

$$k_0 = [(E_Q+\omega_Q)^2+k^2]^{\frac{1}{2}}-M, \quad (4.1)$$

it is clear that, for given electron direction, each final electron energy corresponds to a final pion-nucleon state of unique relative energy $(E_Q+\omega_Q)$. The differential cross section for inelastic scattering (without observation of the resultant pion) therefore has a particularly direct relationship with the desired matrix elements $\mathbf{J}$. In this situation, it is, of course, the total cross section for production of both positive and neutral pions of given ω_Q which is effective.

To discuss this, we return to the differential cross section (2.7),

$$\delta(M+k_0-\omega_q-E_s)\delta(\mathbf{k}-\mathbf{q}-\mathbf{s}) \times\frac{1}{64\pi^4}\Phi_e\frac{\alpha M}{(k^2-k_0{}^2)}\frac{d_3s}{E_s}\frac{d_3q}{\omega_q}\frac{d_3p'}{p\epsilon'}, \quad (4.2)$$

where $k_0=\epsilon-\epsilon'$, $\mathbf{k}=\mathbf{p}-\mathbf{p}'$, and Φ_e is the expression (2.11). It is naturally convenient to transform the nucleon and pion variables to their c.m. system. Consider

$$\delta(M+k_0-\omega_q-E_s)\delta(\mathbf{k}-\mathbf{q}-\mathbf{s})\frac{d_3s}{E_s}\frac{d_3q}{\omega_q}. \quad (4.3)$$

This quantity has simple transformation properties for change of Lorentz frame for $\mathbf{s}$ and $\mathbf{q}$; in the pion-nucleon c.m. system it takes the form

$$\delta\{[(M+k_0)^2-k^2]^{\frac{1}{2}}-\omega_Q-E_S\}\delta(\mathbf{Q}+\mathbf{S})\frac{d_3S}{E_S}\frac{d_3Q}{\omega_Q}. \quad (4.4)$$

By integration over $\mathbf{S}$ and $\mathbf{Q}$, this expression (4.4) is reduced to

$$\frac{4\pi Q}{E_Q+\omega_Q}d\bar{\Omega}, \quad (4.5)$$

where $d\bar{\Omega}$ denotes an average over all directions of $\mathbf{Q}$, and Q is given by

$$E_Q+\omega_Q = [(M+k_0)^2-k^2]^{\frac{1}{2}} \quad (4.6)$$

in accord with Eq. (4.1).

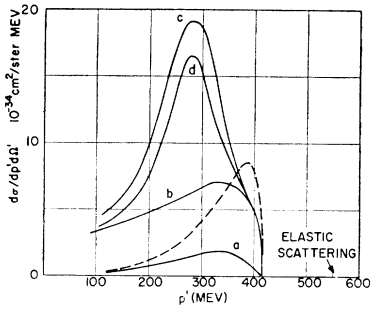

FIG. 3. Spectrum of electrons scattered inelastically off protons. The laboratory angle of scattering is 30° and the incident electron energy is 600 Mev. The curves plotted are (a) Longitudinal production (calculated in Born approximation for the fixed-source theory); (b) Total Born approximation result; (c) Result for Chew-Low matrix element (form factor unity); (d) Result for Chew-Low matrix element (empirical magnetic moment form factor). The dashed curve shows the longitudinal contribution for the assumption $D_l=D_t$.

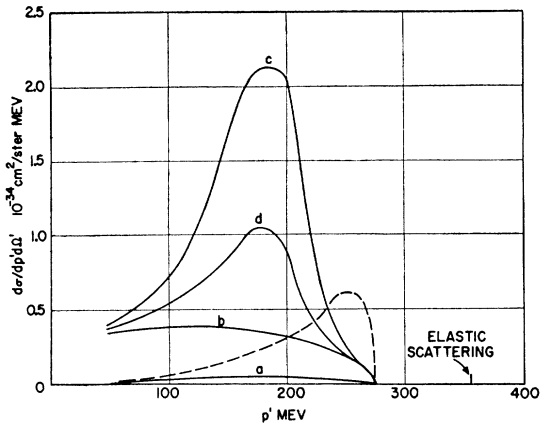

FIG. 4. Results for the same cases as Fig. 3 for a laboratory scattering angle of 90° and incident electron energy of 600 Mev.

For the final integration it is naturally convenient to express Φ_e in terms of c.m. variables: Φ_e is expressed in terms of the laboratory current matrix element $\mathbf{j}$ by Eq. (2.11), and the components of $\mathbf{j}$ are related to the components of the c.m. current $\mathbf{J}$ by

$$j_t=J_t, \quad j_l=k_0J_l/K_0. \tag{4.7}$$

After averaging over directions of $\mathbf{Q}$, the interference between longitudinal and transverse matrix elements vanishes, with the final result

$$\langle\Phi_e\rangle_{\text{Av}}=\int\Phi_e d\bar{\Omega}$$
$$=2\sum_{ij}\frac{T_{ij}}{(k^2-k_0^2)}\left[\frac{1}{2}\left(\delta_{ij}-\frac{k_ik_j}{k^2}\right)\langle\mathbf{J}_t\cdot\mathbf{J}_t\rangle_{\text{Av}}\right.$$
$$\left.+\frac{k_ik_j}{k^2}\left(1-\frac{k^2}{k_0^2}\right)^2\frac{k_0^2}{K_0^2}\langle\mathbf{J}_l\cdot\mathbf{J}_l\rangle_{\text{Av}}\right], \tag{4.8}$$

where the angular braces $\langle\ \rangle_{\text{Av}}$ denote an average over directions of $\mathbf{Q}$ and over initial nucleon spin orientations, and a sum over final spin orientations. This expression reduces at once to

$$2p^2\left[X\langle\mathbf{J}_t\cdot\mathbf{J}_t\rangle_{\text{Av}}+Y\left(\frac{k_0}{K_0}\right)^2\langle\mathbf{J}_l\cdot\mathbf{J}_l\rangle_{\text{Av}}\right], \tag{4.9}$$

where X and Y are defined by Eq. (3.6). Further, different partial waves no longer interfere: for example, with the matrix elements (3.1), (3.2), and (3.3)

$$\langle\mathbf{J}_t\cdot\mathbf{J}_t\rangle_{\text{Av}}=2|D_t|^2+2|M_1|^2+4|M_3|^2+(4/3)|E_t|^2,$$
$$\langle\mathbf{J}_l\cdot\mathbf{J}_l\rangle_{\text{Av}}=|D_l|^2+|O_l|^2+(8/9)|E_l|^2. \tag{4.10}$$

The total π^+ and π^0 production is obtained, following Eqs. (3.4) and (3.5), by replacement of each X_α^2 in (4.10) by $(X_{\alpha1}^2+X_{\alpha3}^2)$.

For the Chew-Low matrix element, expressions for $\langle\mathbf{J}_t\cdot\mathbf{J}_t\rangle_{\text{Av}}$ and $\langle\mathbf{J}_l\cdot\mathbf{J}_l\rangle_{\text{Av}}$ are given in Eqs. (A.18) and (A.19); the term $|D|^2$ given is to be multiplied by a factor 3 to take account of neutral pion production which has amplitude $\sqrt{2}$ times the expression (3.12). For calculation of the inelastic energy spectrum for this case, an additional factor (K_0/K_{ph}) will be included in J_l for the reasons discussed in Secs. 3b and 3c; here K_{ph} denotes the photon energy necessary in the c.m. system for photoproduction of this final state Q, given by

$$K_{\text{ph}}=[E_Q+\omega_Q-M^2/(E_Q+\omega_Q)]/2.$$

The electron energy spectrum is finally

$$\frac{\alpha}{16\pi^3}\langle\Phi_e\rangle_{\text{Av}}\frac{Qp'}{p(k^2-k_0^2)}\frac{M}{[(M+k_0)^2-k^2]^{\frac{1}{2}}}dp'd\Omega'. \tag{4.11}$$

In Figs. 3 and 4 typical electron spectra for incident energy 600 Mev are plotted for scattering angles $\theta=30°$ and 90°, based on the Chew-Low matrix element. In these diagrams it is shown how the final curve is made up of contributions from longitudinal excitations, resonance excitations and other transverse excitations. Roughly speaking, such a curve depicts (apart from some slowly-varying factors) the total electromagnetic pion-production cross section for a given momentum transfer as a function of the pion-nucleon relative energy.

From the curves of Figs. 3 and 4, it is apparent that, according to the matrix element of Chew and Low, the longitudinal contributions to pion production form only a small part of the total inelastic scattering, especially near the pion threshold. The shape of the longitudinal curve obtained derives from the fact that $D_l\ll D_t$ for large momentum transfers K, so that S-wave pion production is negligible compared with the P-wave production through the monopole transitions O_l, which falls only slowly with large K^2 and is therefore dominant here; however, even the contribution predicted for O_l is never more than 25% of the total inelastic scattering.

The dashed curve depicts the contribution obtained from a longitudinal matrix element D_l equal to the transverse D_t (which is a constant for these large momentum transfers). Observations on the inelastic intensity for final energies corresponding to definite ω_Q near the pion threshold would provide a direct check on the smallness predicted for the longitudinal production and on the validity of the Born approximation for S-wave excitations, as a function of K.

For larger energy losses, it is the excitation of the pion-nucleon resonant state through the enhanced matrix elements which is expected to be dominant. The Chew-Low matrix element does not include any enhanced $E2$ transitions which would add to the contribution of the well-known $M1$ resonance excitation. The importance of this $M1$ excitation for large scattering angles will depend on the magnetic-moment structure function $F(K^2)$, which is generally taken as unity in the Chew-Low expression—the present indications from the analysis of elastic electron-proton scattering,[25] which gives an rms radius of about 0.7×10^{-13} cm for the magnetic-moment structure (Gaussian shape assumed), would suggest that the magnetic excitation for 90° electron scattering would be reduced to about 25% of its value for a point magnetic moment (see Figs. 3 and 4). It seems reasonable to say that observations on inelastic scattering in the resonance region would primarily give information on this magnetic-moment structure function $F(K^2)$. Some uncertainty in $F(K^2)$ would arise from the fact that these observations cannot distinguish between $M1$ excitations and $E2$ resonance excitations which would add to them; however other evidence suggests that the $E2$ excitations are relatively weak in this process so that this uncertainty is probably not of importance.

Thus, information on inelastic electron-proton scattering will be of the greatest interest since it will provide a stringent test, for large momentum transfer, of any theory of the structure of the pion-nucleon system. However, it is also apparent that its analysis and unambiguous separation into the various excitations occurring will be very difficult in the absence of knowledge concerning the angular correlations between pion and virtual photon, and that the guidance of theoretical models will be desirable for its interpretation.

5. RESULTS AND DISCUSSION

Calculations have been carried out for several different combinations of the experimental parameters—incident electron energy and pion angle and energy—and for various models of the process. These combinations of parameters are tabulated in Table II, together with the published experimental results[1] for two of the cases. A summary of the results for the more important theoretical models is presented in Table III. These results were obtained by numerical integration of Eq. (2.13) using Gauss' method; in all cases Φ_e and $\Phi_{\rm ph}$ were evaluated in the pion-nucleon c.m. system. To illustrate how the contributions to N_e depend on the scattering angle of the electron, we have tabulated the integrand of Eq. (2.13) for various models in Table IV. In the phenomenological treatment the simple momentum dependence expected for the X_α's was assumed without any additional "form factor." In Table III, the terms "pure D_t^2," etc., refer to N_e values calculated as though only that particular contribution appeared in Φ_e and $\Phi_{\rm ph}$; this is true also for the quantities appearing in Table IV. In combining these "pure" terms to obtain the "transverse mixture," the values of E_{t3}, M_{33}, and D_t given by Watson *et al.*[19] were used; the interference between D_t and the enhanced contributions is included in this mixture. The additional longitudinal and interference contributions were calculated assuming that $D_l=D_t$, $O_l=D_t$, or $E_l=E_t$; results for other values of D_l, O_l, and E_l may be obtained simply by scaling those given in the tables.

TABLE II. The experimental parameters for which N_e has been computed. The experimental values are from reference 1.

Case	p (Mev)	T_π (Mev)	α	k_f (Mev)	P_f' (Mev)	Experimental N_e
I	600	60	75°	228	372	0.0193±0.0010
II	600	147	75°	361	239	
III	600	170	75°	400	200	0.0155±0.0020
IV	800	170	75°	400	400	
V	1000	170	75°	400	600	
VI	600	36	135°	225	375	
VII	600	70	135°	301	299	
VIII	600	93	135°	362	238	
IX	600	30	45°	178	422	

The theoretical results obtained follow the general pattern expected from the discussion in the introduction. The influence of the recoil of the nucleon and the appropriateness of the use of the matrix elements in the pion-nucleon c.m. system have been repeatedly emphasized and are illustrated by the results of Table I As shown in Table III, the values of N_e for the magnetic dipole and transverse electric quadrupole excitations are somewhat larger than for the transverse electric dipole matrix element; this results of course from the fact that the former matrix elements increase in proportion to K while the latter is independent of the momentum of the virtual photon However, in contrast to the "simplified phenomenological model" of Sec. 2, the magnetic dipole and transverse electric quadrupole matrix elements, as well as their interference contribution, lead to slightly different values of N_e; this was already indicated in the fixed-nucleon approximation (3.6). In principle this allows the possibility of determining the relative magnitudes of these phenomenological coefficients by carrying out experiments at appropriate values of p, ω_q, and α, especially as their relative weight in the net pion production depends strongly on $\cos\alpha$. Several runs carried out at the same photon energy k_f, but various meson angles (with the energy at each angle fixed by the photon energy),

TABLE III. Summary of N_e values for some of the more important theoretical models. The terms "pure D_t^2," etc., refer to N_e values calculated for the assumption that all other phenomenological constants vanish; "transverse mixture" refers to N_e values obtained by using the parameters of reference 19. The additional longitudinal and interference contributions are given for the assumption $D_l=D_t$, $O_l=D_t$, or $E_l=E_t$. In the meson theory results, the two different "Born approx" headings refer to the two ways of treating the longitudinal contribution, as explained in the text.

	I	II	III	IV	V	VI	VII	VIII	IX
					Phenomenological				
Pure D_t^2	0.0200	0.0161	0.0152	0.0184	0.0209	0.0199	0.0173	0.0156	0.0219
Pure M_3^2	0.0238	0.0178	0.0165	0.0206	0.0238	0.0248	0.0201	0.0175	0.0270
Pure E_t^2	0.0247	0.0180	0.0166	0.0210	0.0245	0.0256	0.0206	0.0177	0.0265
Pure E_t-M_3	0.0205	0.0170	0.0160	0.0191	0.0212	0.0261	0.0207	0.0178	0.0404
Transverse mixture	0.0207	0.0167	0.0155	0.0190	0.0219	0.0204	0.0178	0.0159	0.0220
D_l^2	0.0021	0.0006	0.0005	0.0012	0.0018	0.0021	0.0010	0.0005	0.0037
O_l-D_t	−0.0001	0.0003	0.0004	0.0005	0.0005	0.0017	0.0008	0.0004	−0.0041
O_l^2	0.0064	0.0010	0.0007	0.0022	0.0050	0.0082	0.0023	0.0010	0.0145
$(M_3+\frac{1}{3}E_t)-E_l$	0.0002	0.0001	0.0000	0.0001	0.0001	−0.0001	−0.0001	−0.0001	0.0000
E_l^2	0.0001	0.0000	0.0000	0.0001	0.0001	0.0002	0.0002	0.0001	0.0000
					Meson theory				
Chew-Low	0.0217	0.0175	0.0162	0.0203	0.0236	0.0211	0.0177	0.0156	0.0227
Transverse	0.0209	0.0169	0.0157	0.0194	0.0223	0.0206	0.0178	0.0156	0.0226
Longitudinal	0.0005	0.0002	0.0002	0.0004	0.0006	0.0003	0.0001	0.0001	0.0011
Interference	0.0003	0.0004	0.0003	0.0005	0.0007	0.0002	−0.0002	−0.0001	−0.0010
Born approx*	0.0212	0.0170	0.0158	0.0196	0.0224	0.0205	0.0177	0.0159	0.0225
Born approx	0.0218	0.0172	0.0160	0.0201	0.0238	0.0206	0.0178	0.0159	···
Relativistic weak coupling	0.0213	0.0168	0.0157	0.0195	0.0224	0.0204	0.0176	0.0157	0.0225

would in effect determine slightly different combinations of these coefficients. However, the difference between the various enhanced contributions is much smaller than the difference between the enhanced and unenhanced contributions, and it would require very great experimental accuracy to separate out all the effects. Most important of all, no form factors have been included in these phenomenological calculations of Table III; the presence of a form factor for each multipole introduces a greater uncertainty in the theory than the difference between some of the ideal point interaction values for N_e. In fact it would seem best to use measured values of N_e together with information obtained from photoproduction to infer information about the longitudinal contributions and form factors. Such information will always be somewhat ambiguous because a form factor would be expected to decrease the value of N_e while the longitudinal contributions would increase it.

In contrast, a specific meson theory will generally make a quite definite prediction for N_e, so that these experiments can then be considered as a check on this theory. For example, assuming the correctness of our treatment of the longitudinal components in the fixed-source theory, the experimental value of N_e provides a test of the Chew-Low matrix element in a region inaccessible to photoproduction experiments. In Secs. 2 and 3, it has been argued that it is appropriate to modify the longitudinal part of the Born approximation matrix element by a factor (K_0/K_f). Values of N_e for this case have been calculated with and without this factor (the former is labeled "Born approx*" in Table III). Whenever the difference is significant, the former gives the closer agreement with the calculation for relativistic Born approximation, thus providing a check on the discussion of Sec. 3c. Next, it is of interest to compare the Chew-Low and Born-approximation values for case I with the phenomenological treatment, using the Born-approximation values for the coefficients. These have been plotted (for a slightly different energy) in Fig. 1. The principal transverse contribution comes from D_t. Since this increases slightly with K, the transverse part of N_e should be slightly greater than the standard value; it turns out to be 0.0203. The principal longitudinal contributions come from O_l and D_l; these are about one-half of D_t on the energy shell and drop considerably below the energy dependence assumed for the phenomenological treatment ($D_l \propto$ const, $O_l \propto K$). The resulting longitudinal contribution is 0.0006. The remaining Born-approximation contribution of 0.0003 arises from the interference between transverse and longitudinal production; it cannot be attributed to D_l-D_t interference (which always vanishes), or O_l-D_t interference which is small at this energy and angle (the c.m. angle is 91° for forward scattering), but arises from the interference of O_l with the transverse P-wave excitations. The Chew-Low value[27] is further increased above this value (0.0212) to 0.0217 owing to the con-

[27] R. B. Curtis [Phys. Rev. **104**, 211 (1956)] has also calculated values of N_e for cases I and III, based on the Chew-Low matrix element. (We thank Dr. Curtis for sending us a copy of his paper before publication.) His results are, respectively, 0.0220 and 0.0157. The difference between his results and ours arises partly from his use of the Chew-Low matrix directly in the laboratory frame rather than the pion-nucleon c.m. frame, and partly from the comparison of the calculated electropion production (in excess of the standard value) with the empirical photoproduction data rather than with that given by the Chew-Low matrix element (which means that the off-diagonal matrix elements used do not necessarily join smoothly with the photoproduction matrix element).

TABLE IV. The integrand of Eq. (2.13) for Case I for the various theoretical models of Table III. The headings (i), (ii), and (iii) refer, respectively, to the azimuthal angles 30°, 90°, and 150°.

		D_l^2	M_3^2	E_l^2	M_3-E_l	Mixture	D_l^2	O_l-D_l	O_l^2	$(M_3+\frac{1}{2}E_l)-E_l$	E_l^2	Born approx*	Chew-Low
	(i)	428.9	343.3	702.1	676.5	425.1	9.3	−101.0	10.4	1.1	0.1	348.9	393.7
$\theta=4.0°$	(ii)	450.7	710.4	50.7	50.0	476.0	9.9	−3.5	11.0	0.0	0.1	515.4	470.8
	(iii)	474.2	333.5	636.1	623.3	458.0	10.6	102.9	11.6	0.8	0.1	521.7	514.7
	(i)	10.74	15.59	34.64	20.21	11.96	4.74	−13.90	9.65	0.71	0.12	7.14	10.96
$\theta=18.9°$	(ii)	12.54	29.83	4.15	3.20	14.91	5.64	−1.97	9.08	0.02	0.08	15.27	15.90
	(iii)	14.86	13.61	21.99	14.42	14.71	7.16	14.20	8.10	0.45	0.09	29.76	25.72
	(i)	1.16	3.74	8.47	1.85	1.53	1.38	−3.28	6.50	0.35	0.10	0.83	1.71
$\theta=39.1°$	(ii)	1.37	6.20	2.13	0.93	2.13	1.83	−0.61	6.25	0.03	0.06	1.73	2.40
	(iii)	1.64	2.92	3.81	2.68	1.89	2.50	3.40	4.94	0.12	0.05	3.74	3.30
	(i)	0.37	1.87	4.11	0.34	0.63	0.56	−1.35	4.41	0.19	0.07	0.29	0.73
$\theta=55.5°$	(ii)	0.43	2.74	1.54	0.47	0.80	0.74	−0.24	4.01	0.02	0.05	0.54	0.94
	(iii)	0.50	1.41	1.69	1.59	0.68	1.01	1.49	3.10	0.03	0.03	1.03	1.03
	(i)	0.14	1.04	2.15	0.01	0.29	0.21	−0.56	2.17	0.09	0.04	0.12	0.35
$\theta=74.6°$	(ii)	0.16	1.33	1.11	0.25	0.37	0.27	−0.08	2.15	0.01	0.03	0.20	0.42
	(iii)	0.18	0.81	0.95	0.94	0.31	0.37	0.67	1.74	−0.01	0.01	0.34	0.38
	(i)	0.03	0.39	0.70	0.01	0.09	0.02	−0.09	0.27	0.02	0.00	0.03	0.11
$\theta=126.9°$	(ii)	0.04	0.41	0.56	0.09	0.10	0.04	−0.01	0.27	0.00	0.00	0.04	0.12
	(iii)	0.04	0.36	0.48	0.23	0.10	0.02	0.10	0.25	−0.01	0.00	0.05	0.07

tribution of the $M1$ resonance excitation (3.12) and its interference with other transverse terms (this excitation does not interfere with O_l and the D_l-M_3 interference is small at this angle and energy). The separation of the Chew-Low value into transverse, longitudinal, and interference contributions is given for all cases in Table III.

The experimental results of reference 1 may now be compared with these various estimates; only a brief discussion is given since these experiments are being repeated with better statistics and for other experimental parameters. The result for case I lies below the standard value of N_e and significantly below the electric dipole estimate with $D_l=D_t$. It should be noted that moderate form factors in the transverse excitations are rather ineffective in reducing N_e much below the standard value; this follows from the fact that the large momentum transfers whose effect is to be diminished by the form factor already contribute rather weakly in the standard value. Thus, the assumption of an rms radius as large as 10^{-13} cm involves only a 4% decrease in N_e for transverse electric dipole. It may be concluded that longitudinal production contributes relatively little to the observed N_e. The known presence of P-wave excitation in the corresponding photoproduction strengthens this conclusion since these excitations increase the transverse N_e above the standard value. In the Chew-Low theory the resonance excitation increases the transverse N_e to 0.0207; the presence of longitudinal production in this theory increases N_e only by 0.0009. Hence this experimental result appears to provide an indication that the longitudinal matrix elements are small relative to the transverse, and this indication is in qualitative accord with the prediction of pseudoscalar pion theory. An experiment at lower pion energy or more forward angle (essentially, for lower k_f) would be of particular interest to strengthen the conclusion that this specific feature of the theory, the weakness of longitudinal relative to transverse electric-dipole matrix elements, is reflected by the data. For lower k_f, the P-wave monopole excitation will be correspondingly weaker while the value of N_e becomes more sensitive to a given longitudinal matrix element. The result for case III has a considerable statistical error, and the difference between theoretical models is so small that almost any model is compatible with experiment; the experiment could put an upper bound on E_l through its interference with M_3 and E_t.

The effect of varying the incident electron energy for fixed-pion angle and energy (and hence fixed-photon energy) is illustrated by cases III, IV, and V. At the lowest electron energy (600 Mev) the difference between the various models is quite small and they would be hard to distinguish experimentally. At higher incident energies the difference between models becomes pronounced, but a new experimental uncertainty is introduced because of the double-pion correction discussed in reference 1. If the double-pion correction can be made with confidence, it would be best to carry out experiments at the highest available electron energy. This dependence of N_e on the incident energy may be understood qualitatively as follows: When the energy of the scattered electron is small, the longitudinal contributions tend to be decreased relative to the transverse ones; this may be seen by comparing the behavior of X and Y, introduced in Eq. (3.6). In addition, the range of variation of K is reduced so that the transverse matrix elements deviate less from their real photon

values. These two effects tend to make different models less distinguishable for smaller incident energies.

The dependence of the various contributions on electron-scattering angle, given in Table IV, shows some interesting features. The first of these is the general forward peaking of the transverse contributions and the more spread-out nature of the longitudinal contributions as was expected from previous discussions. More striking perhaps is the marked azimuthal asymmetry which occurs for several of the models. This asymmetry is associated with the fact that the virtual photons may be considered to be partially polarized, as mentioned in connection with Eq. (2.16). The asymmetry in the magnetic dipole production indicates that the meson tends to be emitted in the direction of the H vector, while in the electric quadrupole production the preferred direction of emission is along the E vector. Except for slight deviations arising from recoil effects, both of these distributions are symmetrical about $\phi=90°$. In contrast the O_l-D_l interference shows a different type of asymmetry which is roughly proportional to $(-\cos\phi)$. The asymmetry occurring in the Born approximation results primarily from the presence of the O_l contribution. A coincidence experiment which would give the correlation in direction between the meson and the inelastically scattered electron would provide valuable information about the strength of the monopole production. Such an experiment would be very difficult using counter techniques; however, a cloud-chamber experiment which would lead to some information about this angular correlation is now under consideration at Stanford.

6. ACKNOWLEDGMENTS

We wish to thank Professor Wolfgang K. H. Panofsky and Dr. G. B. Yodh for several interesting conversations relating to this work and for informing us of their experimental results before publication. Help with the numerical calculations was provided by Mr. H. M. Fried and Mrs. B. Levine.

APPENDIX

A. Kinematical Relations

We shall discuss here the derivation of the kinematical relations which are necessary for calculating pion production by electrons. The following notation will be employed: Small letters refer to quantities evaluated in the laboratory reference frame and capital letters refer to quantities evaluated in the center-of-mass frame of the virtual photon and the proton (which is of course the same as that of the pion and the neutron). For example, a_μ is the μth component of a four-vector, a is the magnitude of its space part $\mathbf{a}$, and a_0 is its time component, all evaluated in the laboratory frame. The invariant inner product is defined $a_\mu b_\mu = \mathbf{a}\cdot\mathbf{b}-a_0b_0$. The four-momenta of the various particles are as follows: incident electron, p_μ; final electron, p_μ'; pion, q_μ; proton, r_μ; and neutron, s_μ. The four-momentum of the virtual photon is $k_\mu=p_\mu-p_\mu'$. The four-momentum vector for each particle satisfies the usual relation between energy and momentum. The difference in mass between the proton and neutron will be neglected; this introduces a slight error which is negligible in comparison with the other uncertainties in the calculation. Wherever possible the mass of the electron will be neglected in comparison with its energy; This requires some care because of the singular nature of the integrand of Eq. (2.13) in the forward direction.

First we consider the derivation of Eq. (2.14). From energy and momentum conservation we have

$$p_\mu+r_\mu=p_\mu'+q_\mu+s_\mu. \tag{A.1}$$

Expressing the invariant $s_\mu s_\mu=-M^2$ in terms of this equation and evaluating the resulting invariants in terms of the laboratory quantities, we easily find Eq. (2.14). For each electron-scattering angle, this fixes all momenta with which we shall be concerned. We can accordingly evaluate all invariant inner products in terms of laboratory quantities.

In order to evaluate matrix elements in the c.m. frame, we shall frequently need quantities of the form $\mathbf{A}\cdot\mathbf{B}$. Such a quantity may be expressed in terms of the invariant $a_\mu b_\mu$

$$\mathbf{A}\cdot\mathbf{B}=a_\mu b_\mu+A_0B_0. \tag{A.2}$$

Now in the c.m. system, the four-vector $D_\mu=K_\mu+R_\mu$ by definition has no space components ($\mathbf{D}=0$). Accordingly we can write

$$\begin{aligned} A_0&=-A_\mu D_\mu/(-D_\mu D_\mu)^{\frac{1}{2}}\\ &=-a_\mu d_\mu/(-d_\mu d_\mu)^{\frac{1}{2}}. \end{aligned} \tag{A.3}$$

In this way, all the quantities we need can be simply evaluated; we need give no special examples.

B. Phenomenological Calculations

In this section of the Appendix we tabulate the various quantities occurring in Eq. (2.11) which arise from the phenomenological expressions Eqs. (3.1), (3.2), and (3.3). It will be convenient to introduce the following abbreviations for some of the frequently occurring quantities:

$$\begin{aligned} &C_1=\mathbf{Q}\cdot\mathbf{K}/QK;\ C_2=\mathbf{P}\cdot\mathbf{K}/PK;\ C_3=\mathbf{Q}\cdot\mathbf{P}/QP;\\ &V_1=[\mathbf{P}\cdot(\mathbf{Q}\times\mathbf{K})]^2/(QK)^2;\quad V_2=(\mathbf{P}\times\mathbf{K})^2/K^2;\\ &\qquad V_3=[\mathbf{Q}\times(\mathbf{K}\times\mathbf{P})]^2/(QK)^2;\\ &\qquad V_4=(\mathbf{P}\times\mathbf{K})\cdot(\mathbf{Q}\times\mathbf{K})/(K^2Q). \end{aligned} \tag{A.4}$$

Then

$$\begin{aligned} \tfrac{1}{2}\,\mathrm{Tr}(\mathbf{J}_t^*\cdot\mathbf{J}_t)&=2|D_t|^2+2|M_1|^2+(5-3C_1^2)|M_3|^2\\ &+(1+C_1^2)|E_t|^2+4C_1\,\mathrm{Re}[D_t^*(M_1-M_3+E_t)]\\ &+2(1-3C_1^2)\,\mathrm{Re}[M_1^*(M_3-E_t)+E_t^*M_3]. \end{aligned} \tag{A.5}$$

$$\tfrac{1}{2}\,\mathrm{Tr}(\mathbf{P}\cdot\mathbf{J}_t{}^*\mathbf{P}\cdot\mathbf{J}_t)$$
$$=V_2|D_t|^2+V_2|M_1|^2+(3V_1+V_2)|M_3|^2+V_3|E_t|^2$$
$$+2C_1V_2\,\mathrm{Re}[D_t{}^*(M_1-M_3+E_t)]$$
$$+2(3V_1-V_2)\,\mathrm{Re}(M_1{}^*M_3)+2(V_3-2V_4{}^2)$$
$$\times\mathrm{Re}[E_t{}^*(M_1-M_3)]. \quad \text{(A.6)}$$

$$\tfrac{1}{4}\,\mathrm{Tr}(\mathbf{P}\cdot\mathbf{J}_t\mathbf{K}\cdot\mathbf{J}+\text{c.c.})=KV_4$$
$$\times\mathrm{Re}\{-D_t{}^*(M_1-M_3-E_t)+O_t{}^*(D_t+2C_1E_t)$$
$$-2E_t{}^*[\tfrac{1}{3}D_t+C_1(M_1-M_3-\tfrac{1}{3}E_t)]\}, \quad \text{(A.7)}$$

$$\tfrac{1}{2}\,\mathrm{Tr}(\mathbf{K}\cdot\mathbf{J}\mathbf{K}\cdot\mathbf{J})=K^2\{|D_l|^2+|O_l|^2$$
$$+(4/9)(3C_1{}^2+1)|E_l|^2+2C_1\,\mathrm{Re}[D_t{}^*(O_t+(4/3)E_t)]$$
$$+(4/3)(3C_1{}^2-1)\,\mathrm{Re}(O_t{}^*E_t)\}. \quad \text{(A.8)}$$

C. Meson-Theory Calculations

Omitting multiplicative factors (which divide out in the expression for N_e), the current density for positive pion production in the Chew-Low theory may be written

$$\mathbf{J}=\left[\boldsymbol{\sigma}-\frac{\boldsymbol{\sigma}\cdot(\mathbf{Q}-\mathbf{K})(2\mathbf{Q}-\mathbf{K})}{\Omega^2}\right]$$
$$+D(2i\mathbf{Q}\times\mathbf{K}+\mathbf{Q}\boldsymbol{\sigma}\cdot\mathbf{K}-\boldsymbol{\sigma}\mathbf{Q}\cdot\mathbf{K})/QK, \quad \text{(A.9)}$$

where

$$D=(K\mu/Q^2)e^{i\delta_{33}}\sin\delta_{33}D_0, \quad \text{(A.10)}$$

and

$$\Omega^2=(\mathbf{Q}-\mathbf{K})^2+\mu^2. \quad \text{(A.11)}$$

Using this expression, the various terms occurring in Eq. (2.11) are

$$\tfrac{1}{2}\,\mathrm{Tr}(\mathbf{J}_t{}^*\cdot\mathbf{J}_t)=2-4(Q^2\mu^2/\Omega^4)(1-C_1{}^2)$$
$$+4\,\mathrm{Re}D[-C_1+(QK/\Omega^2)(1-C_1{}^2)]$$
$$+|D|^2(5-3C_1{}^2); \quad \text{(A.12)}$$

$$\tfrac{1}{2}\,\mathrm{Tr}(\mathbf{K}\cdot\mathbf{J}{}^*\mathbf{K}\cdot\mathbf{J})=[K^2(Q^2+\mu^2)/\Omega^2]-\mu^2A_K{}^2; \quad \text{(A.13)}$$

$$\tfrac{1}{4}\,\mathrm{Tr}(\mathbf{P}\cdot\mathbf{J}_t{}^*\mathbf{K}\cdot\mathbf{J}+\text{c.c.})=\tfrac{1}{4}\,\mathrm{Tr}(\mathbf{P}\cdot\mathbf{J}{}^*\mathbf{K}\cdot\mathbf{J}+\text{c.c.})$$
$$-\tfrac{1}{2}C_2\,\mathrm{Tr}(\mathbf{K}\cdot\mathbf{J}{}^*\mathbf{K}\cdot\mathbf{J}); \quad \text{(A 14)}$$

$$\tfrac{1}{2}\,\mathrm{Tr}(\mathbf{P}\cdot\mathbf{J}_t{}^*\mathbf{P}\cdot\mathbf{J}_t)=\tfrac{1}{2}[\mathrm{Tr}(\mathbf{P}\cdot\mathbf{J}{}^*\mathbf{P}\cdot\mathbf{J})$$
$$-C_2\,\mathrm{Tr}(\mathbf{P}\cdot\mathbf{J}{}^*\mathbf{K}\cdot\mathbf{J}+\text{c.c.})$$
$$+C_2{}^2\,\mathrm{Tr}(\mathbf{K}\cdot\mathbf{J}{}^*\mathbf{K}\cdot\mathbf{J})], \quad \text{(A.15)}$$

where

$$\tfrac{1}{4}\,\mathrm{Tr}(\mathbf{P}\cdot\mathbf{J}{}^*\mathbf{K}\cdot\mathbf{J}+\text{c.c.})=P\cdot K+\tfrac{1}{2}K^2A_P+\tfrac{1}{2}\mathbf{P}\cdot\mathbf{K}A_K$$
$$-\mu^2A_PA_K+\mathrm{Re}D\,KV_4(Q^2+\mu^2)/\Omega^2; \quad \text{(A.16)}$$

$$\tfrac{1}{2}\,\mathrm{Tr}(\mathbf{P}\cdot\mathbf{J}{}^*\mathbf{P}\cdot\mathbf{J})=P^2+\mathbf{P}\cdot\mathbf{K}A_P-\mu^2A_P{}^2$$
$$+2\,\mathrm{Re}D\,[-(\mathbf{P}\times\mathbf{Q})\cdot(\mathbf{P}\times\mathbf{K})/KQ+KV_4A_P]$$
$$+|D|^2(3V_1+V_2), \quad \text{(A.17)}$$

and

$$A_P=[\mathbf{P}\cdot(2\mathbf{Q}-\mathbf{K})]/\Omega^2,$$
$$A_K=[\mathbf{K}\cdot(2\mathbf{Q}-\mathbf{K})]/\Omega^2. \quad \text{(A.18)}$$

The average of expressions (A.12) and (A.13) over directions $\mathbf{Q}$ in the c.m. frame gives the following results:

$$\int d\bar{\Omega}_Q\tfrac{1}{2}\,\mathrm{Tr}(\mathbf{J}_t\cdot\mathbf{J}_t)=2[1-(\mu^2/K^2)I_1(\Lambda)]$$
$$+\mathrm{Re}D\,[I_0(\Lambda)-I_2(\Lambda)]+4|D|^2, \quad \text{(A.19)}$$

$$\int d\bar{\Omega}_Q\tfrac{1}{2}\,\mathrm{Tr}(\mathbf{J}_l\cdot\mathbf{J}_l)$$
$$=(1+2\mu^2/K^2)(\omega_Q{}^2/2QK)I_0(\Lambda)-(\mu^2/K^2)$$
$$-(\mu^2\omega_Q{}^4/4K^4Q^2(\Lambda^2-1)), \quad \text{(A.20)}$$

where the $I_n(\Lambda)$ are defined in Eq. (3.11).

We consider finally the production of pions according to the relativistic weak-coupling theory. Since now there is no question about which is the best Lorentz frame for the evaluation of Φ_e, we may evaluate it directly in the laboratory frame. The current density has been given in Eq. (3.21), and the quantities occurring in Eq. (2.16) are given by

$$\tfrac{1}{4}\,\mathrm{Tr}(\mathbf{b}\cdot\mathbf{j}\mathbf{b}\cdot\mathbf{j})=[(-4M/D_1{}^2)b^2(q_0D_1+k_0\mu^2)$$
$$+(-8M/D_1D_2)\boldsymbol{\lambda}\cdot\mathbf{b}(q_0\mathbf{k}\cdot\mathbf{b}-k_0\mathbf{q}\cdot\mathbf{b})$$
$$+(2/D_2{}^2)(\boldsymbol{\lambda}\cdot\mathbf{b})^2(q_\mu-k_\mu)^2]/4M^2. \quad \text{(A.21)}$$

$$\tfrac{1}{4}\,\mathrm{Tr}(j_\mu j_\mu)=\{(-8M/D_1{}^2)(q_0D_1+k_0\mu^2-M\mu^2)$$
$$+(8M/D_1D_2)[q_0(2\mu^2+k^2-k_0{}^2)-k_0(3\mu^2+2q_\mu k_\mu)]$$
$$+(2/D_2{}^2)\lambda_\mu{}^2(k_\mu-q_\mu)^2\}/M^2, \quad \text{(A.22)}$$

where

$$D_1=-2Mk_0+k^2-k_0{}^2,$$
$$D_2=-2k_\mu q_\mu+k^2-k_0{}^2, \quad \text{(A.23)}$$
$$\lambda_\mu=(2q_\mu-k_\mu).$$